

Received 25 December 2024; revised 12 February 2025; accepted 28 February 2025. Date of publication 3 March 2025; date of current version 21 March 2025.

Digital Object Identifier 10.1109/OJCOMS.2025.3547615

WiLongH: A Custom Hand-Held Platform for Long-Range HaLow Mesh Networks in Human-to-Human Communication

KAVIN KUMAR THANGADORAI^{1,2} (Member, IEEE), KRISHNA M. SIVALINGAM^{1,2} (Fellow, IEEE), ANSHUL PANDEY¹ (Member, IEEE), KUMAR MURUGESAN¹, AND MADHAN RAJ KANAGARATHINAM^{1,2,3} (Senior Member, IEEE)

¹Secure System Research Center, Technology Innovation Institute, Abu Dhabi, UAE

²Department of Computer Science and Engineering, Indian Institute of Technology Madras, Chennai 600036, India

³Connectivity R&D Department, Samsung R&D Institute India, Bengaluru 560037, India

CORRESPONDING AUTHOR: K. K. THANGADORAI (e-mail: kavin.thangadorai@tii.ae)

ABSTRACT Over the past 25 years, IEEE 802.11 (Wi-Fi) has played a vital role in last-mile Internet connectivity. The Wi-Fi HaLow (802.11ah) standard marks a significant leap, offering long-range, low-power connectivity, particularly suited for Internet of Things (IoT) applications. Operating in sub-1 GHz frequencies, Wi-Fi HaLow extends coverage up to 1 km. However, deploying multi-hop HaLow mesh networks for ground-level Human-to-Human (H2H) communication presents unique challenges, as the standard primarily supports star and tree topologies. This paper introduces the *WiLongH* hand-held platform, designed for long-range Wi-Fi HaLow mesh networks aimed at H2H communication at ground level. Utilizing commercial hardware, open-source software, IEEE 802.11s mesh, and the B.A.T.M.A.N. Advanced Routing Protocol (batman-adv) with custom radio profiles, the platform was tested across various environments, including indoor, outdoor, urban, and multi-level parking settings. Results demonstrate that the platform supports voice call ranges exceeding 1 km and video call ranges up to 800 m in line-of-sight conditions, with throughputs of 420 Kbps and 700 Kbps, respectively. In complex urban environments (300-700 m), it achieved up to 64% success for voice calls and 30% for video calls using a 1 MHz channel bandwidth with two nodes. Connectivity across 3-4 floors in basement parking revealed the need for additional mesh nodes. The platform's multicast audio performance showed near-optimal forwarding, outperforming traditional flooding techniques, with 4-node multi-hop performance tested in outdoor and indoor settings. A dense mesh network setup of 14 nodes in an indoor arena further validated the scalability of the platform. Moreover, the use of a SAW filter in the US band (902-928 MHz) significantly reduced cellular interference, enhancing voice and video call performance by 15-20% and 7-10%, respectively. Additionally, the *WiLongH* platform demonstrated a 33% improvement in battery life compared to conventional long-range Wi-Fi mesh systems.

INDEX TERMS Long range Wi-Fi, mesh networks, IEEE 802.11ah, human-to-human communications, performance evaluation.

I. INTRODUCTION

THE IEEE 802.11 (Wi-Fi) [1] technology has become integral to daily life, marking a significant milestone as we celebrate 25 years of Wi-Fi innovation [2] and its transformative impact. Despite its widespread availability in homes, offices, public spaces, campuses, hotels, and

transportation networks for last-mile Internet access, conventional Wi-Fi networks typically offer shorter ranges, approximately 100 m indoors and 200 m outdoors. To address the growing demand for long-range Wi-Fi connectivity while maintaining power efficiency, IEEE 802.11ah [3], also known as Wi-Fi HaLow, has been introduced. Currently,

TABLE 1. Applications of HaLow mesh networks in various sectors and their importance.

Sector	Applications	Importance of Long-Range HaLow Mesh
Emergency & Disaster	Ground-Level Communication for Rescue, Temporary Mesh Networks	Ensures communication in low or no-network areas; low-power for prolonged use in rugged environments
Agriculture	Field Sensors and Monitoring, Ground-Based Livestock Tracking	Connects widespread, low-power sensors across large fields; long range for continuous data collection
Industrial IoT (IIoT)	Asset Tracking in Large Yards, Ground-Level Safety Monitoring	Provides connectivity across large industrial sites; reliable mesh setup in challenging environments
Smart Cities	Traffic Management Sensors, Street Lighting Control	Connects ground-level urban sensors for real-time data; reduces need for frequent power sources
Environmental Monitoring	Weather and Flood Sensors, Wildlife Conservation	Monitors remote or large areas effectively; minimal infrastructure with extended battery life
Defense	Ground-Level Surveillance, Tactical Communication	Enables communication in remote and tactical areas; reliable, secure, and autonomous mesh connectivity

deployments of 802.11ah are underway, particularly in the Internet of Things (IoT) use cases. Operating in the sub-1 GHz frequency range (below 1 GHz), Wi-Fi HaLow offers enhanced penetration and extended coverage compared to traditional Wi-Fi standards, which operate at higher frequencies (2.4/5/6 GHz).

A. MOTIVATION

Versatility and Challenges of Long Range HaLow Mesh Network Scenarios: Wi-Fi network topologies such as star, mesh, and tree [4] have been well-established in the IEEE 802.11 and Wi-Fi Alliance standards. Predominantly, Wi-Fi deployments leverage a star topology with Access Points (APs) at the center, surrounded by client devices. This approach is also prevalent in HaLow networks, especially for IoT applications, where APs connect multiple clients. However, the star topology falls short in scenarios requiring extended range and robust communication, such as in critical first responder operations [5]. For such demanding applications, a multi-hop mesh network becomes essential, as it creates dynamic, on-demand infrastructures that can adapt to the environment. This capability is notably absent in existing HaLow deployments, which limits their utility in scenarios where coverage and reliability are paramount.

While Machine-to-Machine (M2M) communications involving swarms of drones in Air-to-Air (A2A) and Air-to-Ground (A2G) communications have been considered [6], our focus is on Ground-to-Ground (G2G) based Human-to-Human (H2H) communication within HaLow mesh networks. This approach presents unique challenges, such as reduced throughput and increased latency with each hop, but also offers significant opportunities to extend the reach and adaptability of HaLow networks in critical use cases like first responder scenarios (as illustrated in Fig. 1).

Beyond critical operations, the versatility and cost-effectiveness of mesh networks make them an attractive option for a variety of other scenarios, such as agricultural monitoring, industrial IoT, smart city infrastructure, and defense, where HaLow's ability to provide long-range, low-power connectivity makes it ideal for settings where

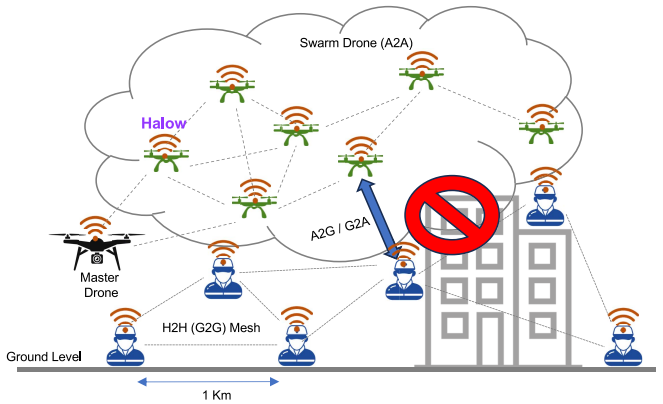


FIGURE 1. A typical scenario for the first responder use case deployment with long-range Wi-Fi HaLow mesh networks.

traditional networks are impractical or too costly. Table 1 highlights the key sectors and applications where HaLow mesh networks can be transformational. This expanded range of use cases demonstrates HaLow's versatility and potential as a future-proof technology. The ability to rapidly deploy a flexible network that can dynamically adjust to environmental conditions is a key advantage of HaLow mesh technology. By addressing these challenges and leveraging the adaptability of mesh networks, our work aims to enhance the deployment and effectiveness of HaLow networks across a wide range of real-world, long-range applications where traditional topologies and technologies may fall short.

Strategic Selection of Wi-Fi HaLow for Sustainable Long-Range Mesh Networks: Selecting the appropriate wireless communication technology is crucial when designing efficient long-range mesh networks. Fig. 2 illustrates the trade-offs between data rate, range, and energy consumption across various wireless technologies from an IoT perspective [7]. This comparison highlights Wi-Fi HaLow's balanced performance, making it an optimal choice for long-range, low-power applications. In many IoT deployments, devices are expected to operate on limited power sources while still delivering consistent performance over long distances. Wi-Fi HaLow meets these needs by offering sufficient data

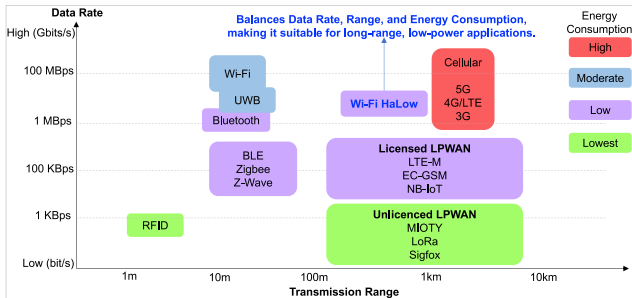


FIGURE 2. Comparison of wireless communication technologies: observing data rate, range, and energy consumption from an IoT perspective, highlighting Wi-Fi HaLow's balance of these factors, making it suitable for long-range, low-power applications.

rates over extended ranges with minimal power consumption, particularly benefiting battery-powered devices in remote or hard-to-reach locations that may not have frequent access to maintenance.

Furthermore, as sustainability becomes a top priority globally, Wi-Fi HaLow's energy efficiency supports the shift toward eco-friendly technologies by reducing power requirements in expansive networks. This technology is particularly suited for applications in sectors like agriculture, where remote monitoring of crop conditions is essential; industrial IoT, for tracking equipment in large facilities; and environmental monitoring, where sensors in remote areas collect data with minimal environmental impact [8]. Thus, the strategic selection of Wi-Fi HaLow tackles key challenges in range, energy efficiency, and data throughput, providing a robust foundation for building efficient, future-proof long-range mesh networks adaptable to a variety of deployment scenarios.

Overcoming Challenges in Ground-to-Ground Wi-Fi HaLow Communications: This section presents experimental studies evaluating the impact of Fresnel Zones (FZ) and antenna height calculations on long-range Wi-Fi HaLow links, with a particular focus on H2H communication scenarios at ground level (illustrated in Fig. 3). In A2A scenarios, where Wi-Fi HaLow links are established between drones, achieving adequate FZ clearance (typically 60% of the first FZ) is generally straightforward. This is because these radio antennas typically operate at significant heights, around 122 m (400 feet), maintaining Line of Sight (LoS) and minimizing concerns beyond Free Space Loss (FSL) and fading. However, H2H communication at ground level introduce significant challenges, particularly in ensuring sufficient FZ clearance [9]. Our calculations using a Fresnel Zone Calculator [10] indicate that to maintain effective Wi-Fi HaLow links over a 1 km range at sub-1 GHz frequencies, antenna heights of approximately 5.4 m (based on 60% Fresnel Zone clearance) are required, a result consistent with the findings of Tschimben et al. [11]. While technically optimal, this height is impractical for H2H communication at ground level, where devices are typically held within 2 m.

Urban environments further complicate H2H communications at ground level due to obstacles like buildings, which create shadowed areas and exacerbate propagation issues. These challenges are technical and practical, as deploying antennas at the required heights may not be feasible in many real-world situations. Overcoming these obstacles is crucial for expanding the applicability of Wi-Fi HaLow networks in densely populated urban areas and other challenging environments. To address these issues, innovative solutions and design optimizations, such as advanced antenna designs, adaptive FZ management techniques [12], and alternative deployment strategies, need to be explored. These approaches could mitigate the challenges of inadequate FZ clearance and urban propagation, ensuring reliable and robust H2H communication at ground level.

Compared to traditional long-range Wi-Fi networks, which often operate at higher frequencies (2.4/5/6 GHz), Wi-Fi HaLow offers distinct advantages in ground level H2H communication scenarios. Traditional Wi-Fi networks face additional challenges, including higher FZ sensitivity, increased Non Line of Sight (N-LoS) propagation issues, and greater susceptibility to interference from other Wi-Fi networks [13]. These factors make traditional long-range Wi-Fi less suitable for robust and resilient communication in H2H communication at ground level, where extended coverage and higher performance are critical.

These challenges underscore the complexity of deploying long-range Wi-Fi HaLow networks in ground level H2H scenarios and highlight the need for continued research and development to overcome the limitations of FZ clearance, antenna height constraints, and urban environments. As illustrated in Table 1, Wi-Fi HaLow's unique attributes make it particularly advantageous for a wide range of real-life applications, such as smart cities, industrial IoT, and agriculture, where traditional networks may struggle due to power limitations, range requirements, or environmental challenges. The IEEE 802.11ah use cases document further highlights these applications, underscoring HaLow's suitability for low-power, long-range IoT deployments in both urban and rural environments [8], [14]. By addressing these challenges, we can extend the benefits of Wi-Fi HaLow to a broader range of applications, including those in urban and densely populated areas where reliable long-range communication is essential.

B. CONTRIBUTION

Despite extensive research on IEEE 802.11ah (HaLow) technologies [15], [16], [17], [18], [19], significant gaps remain in deploying long-range HaLow mesh networks for ground-level H2H communication. This paper addresses these gaps by introducing a custom, headless hand-held platform, *WiLongH*, specifically designed for real-time deployment and performance evaluation of such networks.

The 802.11ah (HaLow) technology provides PHY and MAC enhancements for long-range communication in the sub-1 GHz frequency band. Building on this foundation, we developed a true mesh network architecture using the 802.11s

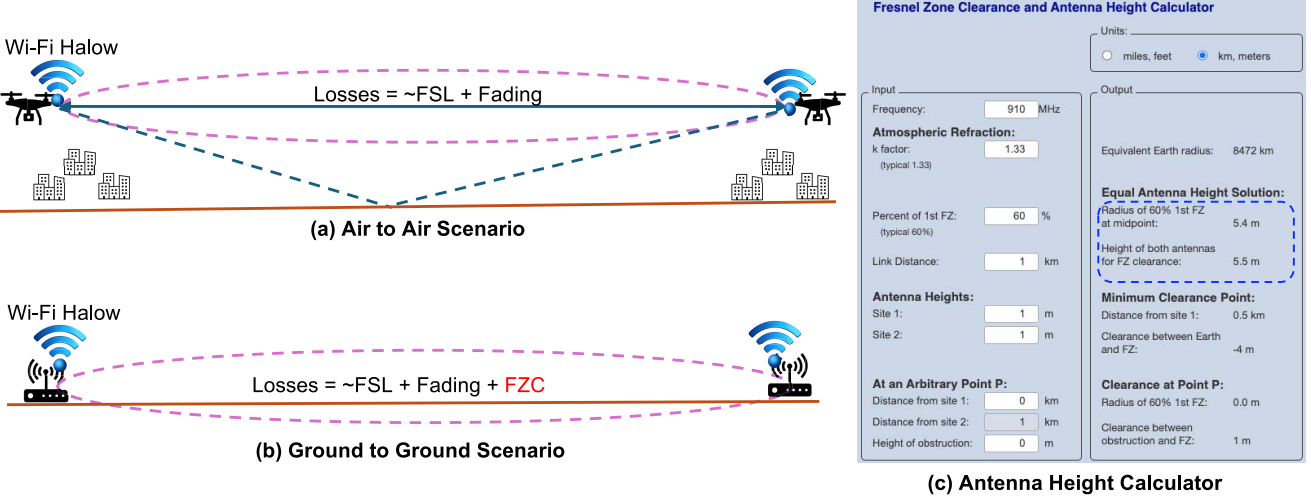


FIGURE 3. (a) Air-to-Air and (b) Ground-to-Ground scenarios for Wi-Fi HaLow with fresnel zone clearance and (c) antenna height calculations, using the fresnel zone calculator online tool for G2G communication.

protocol for neighbor discovery and link establishment. To enhance mobility and flexibility, the default HWMP routing protocol in 802.11s was replaced with B.A.T.M.A.N. Advanced Routing Protocol (batman-adv). This architecture is critical for various applications requiring robust, resilient, and scalable long-range multi-hop networks, as highlighted in Table 1. It enables communication without reliance on centralized nodes or fixed infrastructure, making it suitable for scenarios such as emergency response, industrial IoT, and smart cities.

The key contributions of this research, centered on the *WiLongH* platform, are as follows:

- *Development of a Specialized Hardware and Software Platform:* This research introduces a custom platform combining commercially available hardware and open-source software, enabling long-range HaLow mesh networks for ground-level H2H communication. The platform integrates IEEE 802.11s mesh and batman-adv for scalability in high-mobility scenarios.
- *Design & Development of Unique Radio Profiles:* This research develops custom *WiLongH* radio profiles optimized for long-range Wi-Fi HaLow mesh networks, with tailored PHY and MAC parameters. A comparative long-range Wi-Fi profile was created to validate performance. The *WiLongH* profile, supported by an analytical model, demonstrates effectiveness in low-power, long-range H2H communication.
- *Real-Time Performance Evaluation:* The *WiLongH* platform is designed to be portable, durable, and energy-efficient, ideal for real-time field deployment in challenging environments. Field tests, including LoS and N-LoS assessments, indoor multi-floor evaluations, and dense mesh tests with 14 nodes, demonstrated stable connections over 1 km per mesh hop, with suitable throughput and latency for H2H communication.

- *Addressing Real-Time Deployment Challenges:* We demonstrated the *WiLongH* platform's ability to mitigate cellular interference in the 902-928 MHz US band using a Surface Acoustic Wave (SAW) Band Pass Filter, which reduced interference with a minor trade-off in the link budget. Additionally, the platform's energy efficiency highlights its suitability for long-range, low-power IoT applications.

The subsequent sections of this paper are organized as follows: Section II covers background and related work on HaLow technology and the importance of long-range HaLow mesh networks for ground-level H2H communication. Section III discusses the design of the *WiLongH* platform, including hardware, software, and custom radio parameters, supported by an analytical model. Section IV details the test environments, experiments, and results. Finally, Section V summarizes the findings and suggests future research directions.

II. BACKGROUND AND RELATED WORK

IEEE 802.11ah, commonly known as Wi-Fi HaLow, has emerged as a promising standard for the next generation of the Internet of Things (IoT) due to its long-range connectivity and support for numerous low-power devices. The standard introduces advanced features like the Restricted Access Window (RAW) and Hierarchical Traffic Indication Map (HTIM), which enhance scalability and energy efficiency, making it highly suitable for large-scale IoT deployments.

However, IEEE 802.11ah primarily supports a star topology, where devices communicate directly with a central access point (AP). While optimizing energy efficiency and reducing complexity in dense network environments, this design poses constraints for mesh networks. Though the standard includes a relay-based architecture allowing range extension via intermediate relay nodes, it falls short of

supporting a fully decentralized mesh network, where nodes can communicate directly with each other.

To overcome these constraints, recent research has explored custom adaptations of the IEEE 802.11ah standard to introduce mesh-like features. Enhancements to the MAC layer [3], such as enabling multi-hop communication, have been proposed. However, these adaptations are typically limited to two-hop scenarios [20] and do not fully realize the decentralized, multi-path communication characteristic of true mesh networks.

Several studies have analyzed IEEE 802.11ah but remained focused on star topology, without addressing its applicability for mesh networking. Tian et al. [20] and Enriko and Gustiyana [21] surveyed Wi-Fi HaLow's capabilities for IoT applications, highlighting key research areas yet overlooking mesh networking aspects. Tschimben et al. [11] demonstrated IEEE 802.11ah's long-range feasibility via an SDR-based testbed but limited their study to single-hop communication. Similarly, Maudet et al. [22], [23] conducted real-world HaLow performance evaluations, yet their work remained within a star topology scope. Fayyaz et al. [24] compared IEEE 802.11s and 802.11ah for IoT but did not explore mesh integration for long-range H2H communication.

While some works have examined Wi-Fi mesh networking, they primarily focus on specific applications rather than continuous long-range H2H communication. Anas et al. [25] investigated batman-adv mesh networks for outdoor event settings, and Ashraf et al. [26] studied Wi-Fi mesh for disaster response in resource-constrained environments, yet neither addressed the challenges of HaLow-based long-range mesh networks.

Other studies have explored long-range communication in specialized domains. Unni et al. [27] proposed a long-range Wi-Fi backhaul for over-the-sea communication, while Nilsson and Deknache [28] and Cilfone et al. [29] focused on Bluetooth mesh and seamless handover in Wi-Fi mesh, respectively. However, their findings are not directly applicable to long-range HaLow mesh for H2H communication. A summary of these related works and their limitations in relation to our *WiLongH* platform is provided in Table 2.

Mesh networks, characterized by their decentralized nature that allows direct node-to-node communication, are inherently more resilient to node failures and provide better coverage in challenging environments. The reliance on a star topology limits the flexibility and scalability of networks requiring dynamic and autonomous reconfiguration—key advantages of mesh topologies.

In developing *WiLongH*, a custom HaLow-based long-range mesh network, we address these limitations by extending the capabilities of Wi-Fi HaLow to support mesh networking. This involves creating custom protocols and architectural modifications to enable multi-hop communication and dynamic routing between nodes, thereby overcoming the star topology constraints of the standard. *WiLongH* represents a significant advancement in this

domain, combining theoretical innovations with practical implementations of a HaLow-based mesh network. By modifying both hardware and software components, *WiLongH* demonstrates the feasibility of building a scalable, long-range mesh network using IEEE 802.11ah despite its native focus on star topology.

Deploying HaLow networks on a large scale, particularly in mesh configurations, presents challenges such as efficient network setup, maintenance, and management in environments with minimal infrastructure. These challenges are especially pertinent in ground-level H2H communication scenarios, where the flexibility and resilience of a mesh network are critical.

III. PROPOSED *WiLongH* HAND-HELD PLATFORM FOR H2H LONG-RANGE HaLow MESH NETWORK

A. OVERVIEW OF THE *WiLongH* PLATFORM

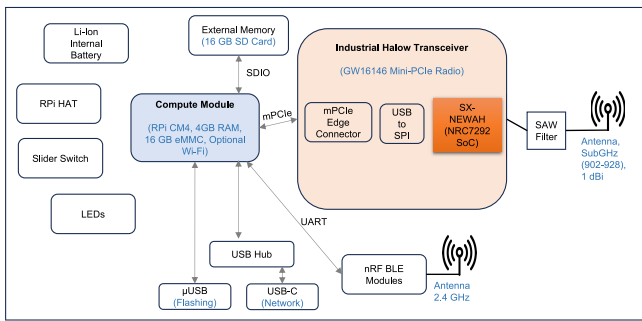
We present *WiLongH*, a specialized hand-held platform developed for constructing long-range Wi-Fi HaLow mesh networks within the license-exempt sub-1 GHz band. Aimed at H2H communication, especially in G2G scenarios, our platform integrates Commercial off-the-shelf (COTS) hardware and open-source software components. These components include the 802.11s mesh link and batman-adv, as detailed in this section.

B. HARDWARE COMPONENT & ASSEMBLY

The hardware architecture is centered on the Raspberry Pi Compute Module 4 (RPi CM4 or RPi CM4 Lite) [30], mounted on a Printed Circuit Board (PCB), featuring 4GB RAM, 16GB eMMC storage, and an optional Wi-Fi radio that supports the 2.4 and 5 GHz bands with IEEE 802.11 a/b/g/n/ac standards [31]. This built-in Wi-Fi radio can serve as a short-range Wi-Fi access point for other clients to connect to the *WiLongH* platform, thereby leveraging the long-range HaLow mesh network and its services. Our design includes a COTS Industrial HaLow Transceiver (GW16146 802.11ah HaLow WiFi Mini-PCIe Radio) [32]. Operating within the sub-1 GHz license-exempt band (US regulatory: 902 - 928 MHz ISM band), this transceiver uses the mPCIe form factor to connect with RPi CM4 with an added USB-SPI bridge atop the SX-NEWAH(US) [33] module. It supports a single spatial stream 802.11ah WLAN, based on the Newracom NRC7292 System-on-Chip (SoC) [34], offering PHY data rates from 150 Kbps up to 15 Mbps, with channel widths of 1/2/4 MHz and a short guard interval. The transceiver delivers up to 23 dBm Tx power (200 mW) and -106 dBm Rx sensitivity. However, the achievable data rate is limited to 4 Mbps due to the constraints of the GW16146 module, with latency reduced by the SPI-USB bridge [35]. To mitigate cellular interference in the US band (902-928 MHz), the HaLow transceiver is paired with an external SAW Band Pass Filter CBPFS-0902 [36], followed by connection to the sub-1 GHz antenna W1063M [37], which provides an average Tx gain of 1 dBi.

TABLE 2. Summary of related work and their limitations with respect to *WiLongH*.

Category	Reference	Work Summary and Limitations
Survey and Review	[20]	Tian et al. provided a comprehensive survey on 802.11ah, identifying research areas such as PHY layer enhancements, fast authentication, and network security. <i>Limitation: Focused on star topology, no exploration of mesh networks for H2H communication.</i>
	[21]	Enriko and Fikri reviewed the potential of Wi-Fi HaLow for agriculture and smart cities, particularly in Indonesia. <i>Limitation: Primarily focused on star topology and IoT applications, no consideration of mesh network deployment.</i>
Real-Time Evaluation	[22]	Maudet et al. conducted real-time evaluation of Wi-Fi HaLow, demonstrating up to 1 km range with 23 dBm transmit power and throughput of around 6 Mbps using a 2 MHz bandwidth. <i>Limitation: No focus on mesh networking or H2H communication.</i>
	[23]	Maudet et al. further explored the energy efficiency of HaLow devices, confirming the technology's promise for low-power, high-throughput applications. <i>Limitation: Limited to star topology, did not address long-range mesh networks.</i>
	[25]	Anas et al. conducted a comprehensive study on the deployment of Wi-Fi mesh networks in outdoor event settings, focusing on the batman-adv. <i>Limitation: Focused on Wi-Fi mesh for outdoor events, did not explore the implications of long-range mesh for H2H communication.</i>
	[11]	Stefan et al. conducted real-world performance evaluation of IEEE 802.11ah using an SDR-based testbed, demonstrating connectivity up to 1 km and analyzing Fresnel Zone impact. <i>Limitation: Limited to single-hop communication, no exploration of mesh networking.</i>
Comparative Analysis	[24]	Fayyaz compared 802.11s (mesh) and 802.11ah (HaLow) standards for IoT, providing insights into their strengths and limitations. <i>Limitation: Did not address coexistence of technologies or relevance to long-range HaLow mesh networks for H2H communication.</i>
	[26]	Asraf et al. investigated Wi-Fi mesh networks for disaster response, emphasizing design considerations for resource-limited settings in developing countries. <i>Limitation: Focused on disaster response, limited exploration of long-range mesh networks for continuous H2H communication.</i>
Over-the-Sea Communication	[27]	Unni et al. proposed a hierarchical point-to-multipoint backhaul network using long-range Wi-Fi for over-the-sea communication, optimizing transmission power, antenna tilt, and channel bandwidth. <i>Limitation: Focused on over-the-sea communication, with limited exploration of terrestrial long-range mesh networks for H2H communication.</i>
Battery-Powered Sensors in Mesh Networks	[28]	Nilsson et al. investigated the use of Bluetooth mesh for battery-powered sensors. <i>Limitation: Did not focus on Wi-Fi or long-range mesh networks.</i>
	[29]	Cilfone et al. explored seamless handover in Wi-Fi-based long-range mesh networks. <i>Limitation: Limited focus on H2H communication scenarios.</i>

**FIGURE 4.** *WiLongH* hardware components: compute module, industrial HaLow transceiver for long-range communication in sub-1 GHz, and additional components.

In addition to the compute module and the HaLow transceiver, the *WiLongH* platform includes several supplementary components as shown in Fig. 4. These components comprise an SD card slot providing 16 GB of secondary

memory when RPi CM4 lite is used, a removable Li-Ion battery with a capacity of up to 5000 mAh, and a slider switch for power control, with LEDs indicating battery level. USB interfaces load custom software onto the *WiLongH* platform and support networking options such as SSH (Secure Shell). Moreover, an nRF BLE module is included for off-channel communication among mesh nodes when the HaLow network is disrupted by interference or jamming. These components collectively form a portable, headless device designed for H2H long-range HaLow mesh communication at ground level.

Next, we describe the hardware assembly of the selected components on the front side of the *WiLongH* in-house PCB, as illustrated in Fig. 5. The baseboard houses the RPi CM4 (or RPi CM4 Lite) in the designated slot, with the GW16146 HaLow module inserted into an available mPCIe slot. Within the GW16146 module, connectivity is established via a UFL to SMA cable, followed by the attachment of the sub-1 GHz

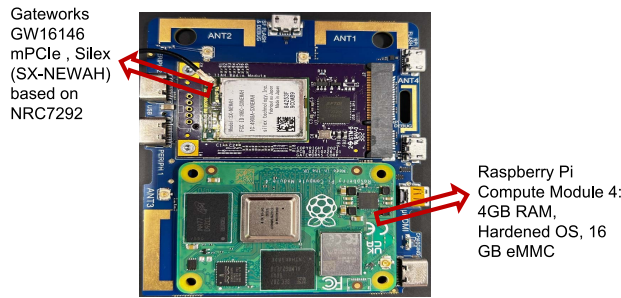


FIGURE 5. *WiLongH* hardware assembly: the raspberry Pi compute module 4 (RPI CM4 or RPI CM4 lite) and GW16146 802.11ah HaLow WiFi mini-Pcie radio securely connected to the baseboard.

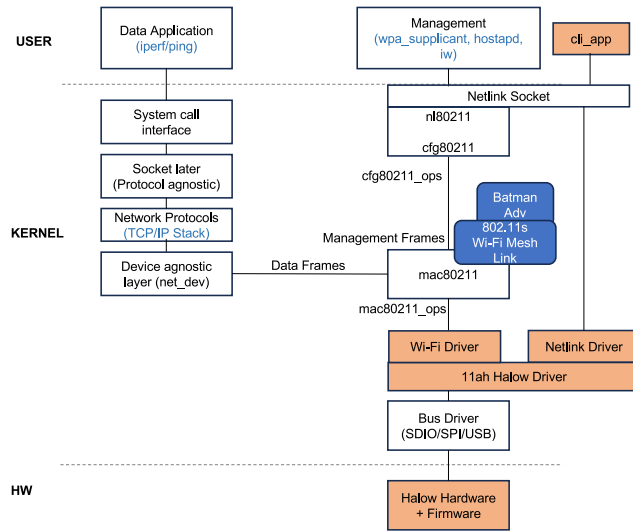


FIGURE 6. *WiLongH* software architecture: The software architecture features separate management and data paths within the Linux Wi-Fi subsystem in secure and robust OS, utilizing Linux Kernel 5.15 with docker, utilizing the 11ah HaLow driver alongside the 802.11s mesh link, batman-adv, and a custom user-level application, *cli_app*.

antenna W1063M after the external SAW filter. Notably, certain hardware components, such as battery connections, thermal pads, and switches, are not discussed as they fall beyond the scope of this paper.

C. SOFTWARE ARCHITECTURE

From a software perspective, our *WiLongH* platform is constructed on a secure and robust OS, utilizing Linux Kernel 5.15 alongside a custom package manager (Docker). We employ the NRC7292 host driver (11ah HaLow driver) [38], which seamlessly integrates with the Linux Wi-Fi subsystem to manage management and data paths independently, as illustrated in Fig. 6. We have integrated an 802.11s protocol stack built on these subsystems for mesh operations [39], facilitating functions such as neighbor discovery and link establishment at the MAC layer (Layer 2). Given that our *WiLongH* platform is primarily used in hand-held headless devices with mobility, we have disabled the default HWMP (Hybrid Wireless Mesh Protocol) routing within the 802.11s software, which is inefficient for mobility [40].

TABLE 3. Radio parameters (profile): *WiLong-LR* and *WiLongH*.

Radio Parameters	Long Range Wi-Fi Configuration (<i>WiLong-LR</i>)	Long Range HaLow Configuration (<i>WiLongH</i>)
Module	Doodle Labs NM-DB-3U	Silex SX-NEWAH
Antenna	3 Linx ANT-DB1-RAF-SMA	Pulse W1063M 868-928 MHz 1.0 dBi + SAW filter
Tx Power	27 dBm	23 dBm
Rx Min Sensitivity	-97 dBm	-106 dBm
MCS	Dynamic (MCS0-MCS23)	Dynamic (MCS0-MCS7)
Min. Data Rate	1.6 Mbps	1.35 Mbps
Min. Throughput	0.96 Mbps	0.67 Mbps
Max. Data Rate	97.5 Mbps	13.5 Mbps
Max. Throughput	58.5 Mbps	6.75 Mbps
MIMO Configuration	MIMO (3x3:3)	SISO (1x1:1)
Coverage Class	3000	NA
RTS/CTS	Disable	Disable
Frequency	5825 / 2442 MHz	902-928 MHz
Preamble	Long (128 bit long)	Long (80 bit long)
Guard Interval	Long (0.8 us)	Long (8 us-10x)
Channel Bandwidth	5/10 MHz	1/2/4 MHz
PHY Standard	802.11n	802.11ah

Instead, we have enabled the batman-adv [41], designed for high mobility scenarios [42]. This protocol enables efficient and robust mesh networking, which is essential for our *WiLongH* platform. Key features include decentralized routing, automatic route selection and maintenance, real-time link quality estimation, minimal overhead, and optimized traffic handling. A custom user-level application, *cli_app* [43], interacts with the 11ah HaLow driver and hardware via netlink socket for configuration tasks (such as adjusting Tx power and operation mode) and for collecting statistics like monitoring channel quality.

D. HaLow RADIO PARAMETERS (PROFILE)

We have established a unique *WiLongH* profile detailing long-range HaLow radio parameters, as shown in Table 3, in comparison with the long-range Wi-Fi radio parameter *WiLong-LR* [44]. These parameters include the module (Silex SX-NEWAH), antenna (Pulse W1063M) with SAW filter, Tx power (23 dBm), channel bandwidth (1/2/4 MHz), and frequency range (902-928 MHz), as previously mentioned. Additionally, we have enabled a dynamic MCS (rate control algorithm) aligned with the NRC7292 host driver and firmware support. This configuration ensures optimal data rates relative to the channel bandwidth, balancing Tx power and Rx sensitivity settings. For example, when two HaLow nodes are in close proximity with a channel bandwidth of 1 MHz, MCS 7 is applied, as described in the Full MCS Table (sub 1 GHz) in [45], resulting in a Tx power of 14 dBm and Rx sensitivity of -85 dBm, with a maximum data rate of

13.5 Mbps. Conversely, under the same configuration with MCS 0, when nodes are distant or environmental conditions are suboptimal, a lower data rate of 1.35 Mbps is achieved with a Tx power of 23 dBm and Rx sensitivity of -102 dBm. To minimize performance overhead, RTS/CTS is disabled. At the same time, a long preamble is adopted for enhanced synchronization, and a long guard interval is employed to improve resilience against multipath interference in long-range communication. For comparison, based on our previous work [44], we configured long-range Wi-Fi using the Doodle Labs NM-DB-3U module [46], termed *WiLong-LR*, operating in the 2.4/5 GHz bands with customized 5/10 MHz channel bandwidths.

In summary, *WiLongH*'s long-range HaLow radio parameters are carefully selected to optimize for long-range, low-power, and robust communication in sub-1 GHz bands, which are essential for applications like H2H communication in first responder use cases at ground level, IoT, and rural connectivity. These choices contrast with *WiLong-LR*'s focus on higher data rates and throughput in higher frequency bands, typical of Wi-Fi systems.

E. ANALYTICAL MODEL FOR *WiLongH* RADIO PARAMETER SELECTION

1) LINK BUDGET ANALYSIS

The link budget equation is essential for understanding the trade-offs between transmit power, antenna gain, and receiver sensitivity. These are critical for achieving long-range communication with the *WiLongH* profile.

$$\text{Link Budget} = P_t + G_t + G_r - L_p - N_f - L_m \quad (1)$$

where:

- P_t is the transmit power, measured in dBm, varying based on MCS, with a maximum of 23 dBm at MCS0.
- G_t and G_r are the transmit and receive antenna gains, measured in dBi. The average gain for the Pulse W1063M 868-928 MHz antenna is 1 dBi; however, the SAW filter introduces a loss of 2.4 dB on both the transmit and receive sides.
- L_p is the path loss, measured in dB, calculated in the subsequent section.
- N_f is the noise figure of the receiver, measured in dB, and also calculated in the following section.
- L_m represents additional losses, such as cable and connector losses, measured in dB, with an expected loss of approximately 1 dB in our platform. Additionally, wireless channel losses are considered as follows:
 - *Polarization Mismatch*: A 1 dB loss occurs due to imperfect alignment between the transmit and receive antennas' polarization, a common issue in real-world deployments.
 - *Fresnel Zone Effect*: A 3 dB loss is introduced due to obstructions or reflections within the Fresnel zone, which can significantly impact signal strength and quality over long distances.

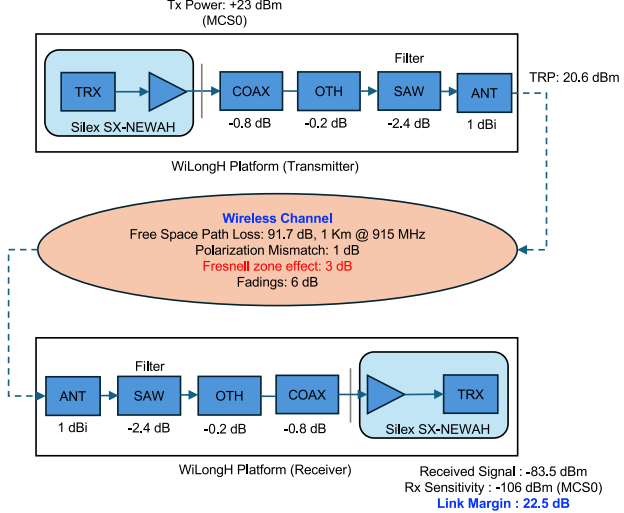


FIGURE 7. Link margin estimation for the *WiLongH* platform at 915 MHz over a 1000 m range using MCS0, accounting for all components, including wireless channel effects.

- *Fading*: A 6 dB loss accounts for multipath fading, where signals arrive at the receiver with varying amplitudes and phases due to reflections, scattering, and diffraction in the environment.

We conducted a detailed link margin estimation for the *WiLongH* platform operating at 915 MHz over a 1000 m range under various configurations, as represented in Fig. 7. From this analysis, we obtained a Link Margin of 22.5 dB, demonstrating the feasibility of long-range communication under the specified conditions.

2) PATH LOSS MODEL

Even though multiple models were proposed by the TGah Task Group [47] to define realistic propagation conditions, we adopted the TGah Urban Micro (UMi) Model for further analysis. This model is designed for urban deployments with moderate building density and ground-level communication. Path loss includes both LoS and NLoS (non-LoS) cases, which are aligned with the *WiLongH* platform analysis. For this model, the path loss is given by:

$$L_p(d) = L_0 + 10n \log_{10}(d) + X_\sigma \quad (2)$$

where:

- L_0 is the path loss at the reference distance (e.g., 1 m).
- n is the path loss exponent, with typical values of 2.5 for LoS and 3.5 for NLoS in UMi environments.
- d is the distance between the transmitter and receiver, and the maximum communication range is subsequently calculated.
- X_σ is the shadow fading component, modeled as a Gaussian random variable with standard deviation σ (4 dB for LoS, 8 dB for NLoS).

In the *WiLongH* platform, the lower frequency sub-1 GHz band (902-928 MHz) significantly reduces path loss compared to higher frequency profiles like *WiLong-LR*, which

typically operate at 2.4 or 5 GHz. This reduction in path loss enables extended communication ranges and improves overall energy efficiency. This characteristic makes *WiLongH* particularly advantageous in long-range, low-power applications, as lower frequencies attenuate less over distance in free-space environments.

Along with the path loss model, the maximum achievable communication range of the *WiLongH* platform is estimated as:

$$d_{\max} = \left(\frac{P_t G_t G_r \lambda^2}{(4\pi)^2 S} \right)^{\frac{1}{\alpha}} \quad (3)$$

where:

- λ : Wavelength, given by $\lambda = \frac{c}{f}$, where c is the speed of light and f is the operating frequency.
- α : Path loss exponent, which varies by environment. In rural or open environments, α is typically around 2, while in urban areas with more obstructions, α can be up to 4.

The combination of a lower frequency band (resulting in a larger wavelength, λ) and reduced path loss exponents allows *WiLongH* to achieve significantly longer communication ranges compared to higher frequency systems. A comparative analysis between *WiLongH* and traditional long-range Wi-Fi (*WiLong-LR*) shows that in urban environments, *WiLongH* achieves a maximum range of 688.6 m, compared to 209.6 m for *WiLong-LR*.

Under the TGah UMi model, a path loss exponent of 3 is a reasonable choice for urban environments, particularly in evaluating Wi-Fi HaLow (*WiLongH*) against traditional long-range Wi-Fi (*WiLong-LR*). Using this value, *WiLongH* achieves a range of 2046.4 m, whereas *WiLong-LR* is limited to 510.9 m. In rural environments, *WiLongH* achieves a range of 9401.4 m, compared to 1778.7 m for *WiLong-LR*. This improvement is attributed to the lower operating frequency and better receiver sensitivity of the *WiLongH* system, making it ideal for long-range, low-power applications.

Further measurements across diverse environments, including urban, rural, and mixed scenarios, are planned to fine-tune model parameters and optimize performance evaluation for *WiLongH* applications, leveraging the well-established TGah models.

3) NOISE FIGURE AND SENSITIVITY

The noise figure N_f measured in decibels (dB), representing additional noise introduced by the receiver, is calculated using the following equation:

$$N_f = S + 174 - 10 \log_{10}(B) - S_{\min} \quad (4)$$

where:

- S is the receiver sensitivity of HaLow radio (SX-NEWAH) used in *WiLongH* platform, it is -106 dBm.

- B is the bandwidth in MHz. In the *WiLongH* profile, we utilize narrow channel bandwidths of 1/2/4 MHz.
- S_{\min} is the minimum required signal-to-noise ratio for reliable communication, expressed in dB. Experimental findings indicate that a minimum SNR of 9 dB is necessary for reliable HaLow communication in voice and video call applications (refer to Section IV-A for test details). For instance, with a 2 MHz channel bandwidth, achieving at least MCS0/1 (optimized for low SNR environments) with an RSSI of -97 dBm (corresponding to 9 dB minimum SNR) ensures a PHY rate of up to 1 Mbps. This SNR value aligns with the application requirements, as a minimum throughput of 1 Mbps is necessary for uninterrupted voice and video communication.

In the *WiLongH* platform, the choice of narrow bandwidths (1/2/4 MHz) and a noise figure N_f optimized for low-power operation results in a sensitivity of -106 dBm. This high sensitivity is critical for supporting long-range communication while maintaining low power consumption, especially in environments with sub-1 GHz frequencies and low data rates.

4) ENERGY EFFICIENCY

The energy per bit E_b is related to the transmit power P_t and the data rate R by:

$$E_b = \frac{P_t}{R} \quad (5)$$

For long-range HaLow communication, P_t is influenced by the path loss $L_p(d)$, as described in Section III-E.2, which depends on the distance d , frequency f , and environment, and base transmit power P_b . Thus, the transmit power for long-range HaLow can be expressed as:

$$P_t = P_b \cdot L_p(d) \quad (6)$$

The data rate R for HaLow radio is determined by the channel bandwidth and the MCS:

$$R = C \cdot M \quad (7)$$

where:

- C : Channel bandwidth (e.g., 1 MHz for HaLow).
- M : Bits per symbol, depending on modulation (e.g., BPSK, QPSK) and coding rate.

For long-range HaLow, narrower bandwidths result in lower data rates, slightly increasing E_b . However, this is offset by reduced P_t due to lower path loss at sub-1 GHz frequencies, making *WiLongH* energy efficient for applications like battery-operated mesh nodes and IoT devices. Additionally, energy overheads (E_o) for mesh communication include control message exchanges, idle listening, and retransmissions, which are significant in long-range HaLow mesh networks. The total energy per bit, accounting for overhead, is given by:

$$E_b = \frac{P_t}{R} + \frac{E_c + E_i + E_{rt} + E_r}{B} \quad (8)$$

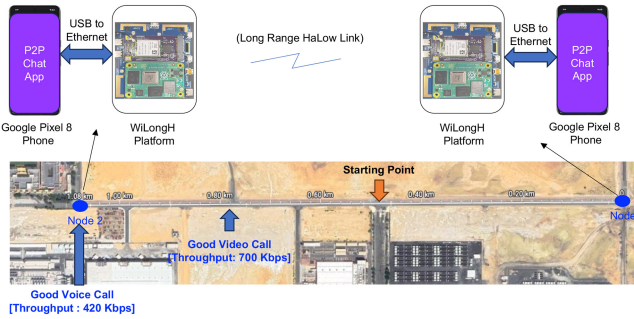


FIGURE 8. Illustration of maximum range test with voice and video call performance results (two nodes - *WiLongH* platform connected to google pixel 8 phones via USB-to-Ethernet adapter): both nodes started at the same location and moved away from each other while monitoring voice and video call performance over HaLow radio. Node 1 was fixed at one corner of the open street, while node 2 continued moving away. Video calls ceased at approximately 800 m, achieving a throughput of around 700 Kbps, while voice call distortion began beyond 1 km with a throughput of around 420 Kbps.

where:

- E_c : Energy spent on batman-adv control messages and beaconing.
- E_i : Energy consumed during idle listening.
- E_{rt} : Energy due to retransmissions in lossy environments.
- E_r : Energy for routing table updates and neighbor discovery.
- B : Total transmitted data (bits).

The energy efficiency directly impacts battery lifetime T_{batt} , which is calculated as:

$$T_{batt} = \frac{B_{cap} \cdot V_{batt} \cdot 3600}{P_{tx} \cdot \alpha_{tx} + P_{rx} \cdot \alpha_{rx} + P_{idle} \cdot \alpha_{idle}} \quad (9)$$

where:

- B_{cap} : Battery capacity in mAh.
- V_{batt} : Battery voltage in volts.
- $\alpha_{tx}, \alpha_{rx}, \alpha_{idle}$: Fractional time spent in transmit, receive, and idle states.
- P_{tx}, P_{rx}, P_{idle} : Power consumption in respective states.

In contrast, traditional long-range Wi-Fi, *WiLong-LR*, operates at higher frequencies (2.4/5 GHz) with wider bandwidths, requiring higher transmit power to compensate for increased path loss, resulting in higher energy per bit.

IV. RESULTS AND DISCUSSIONS

This section evaluates the performance of the *WiLongH* platform across various scenarios by employing unique *WiLongH* profiles and, where relevant, comparing them against the *WiLong-LR* profile.

A. MAXIMUM RANGE EVALUATION (LOS)

To evaluate the maximum range of the *WiLongH* platform's long-range HaLow radio, we conducted tests in an open area (LoS), as shown in Fig. 8, with 2 MHz channel bandwidth. Each of the two nodes in this setup consisted of a Google Pixel8 phone [48] connected to the *WiLongH* headless platform using a USB-to-Ethernet cable. The evaluation

began with both nodes positioned at the same starting point, where they moved apart gradually, monitoring voice and video call performance using our P2P chat application running on the Pixel8 phone. Airplane mode was enabled on each Pixel8 phone to ensure that communication occurred solely via the *WiLongH* platform's HaLow radios, without relying on any Internet connection.

This P2P chat application (unicast traffic), built on the open-source Element platform [49], utilizes the Dendrite Matrix server [50] for decentralized communication and the WebRTC protocol [51] (using UDP transport layer) to support real-time voice and video calls over a peer-to-peer connection. This setup allows us to assess real P2P voice and video call performance over the HaLow radio in the *WiLongH* platform, independent of any external servers or Internet dependency. This application requires a minimum of 200 Kbps for voice and over 700 Kbps for video call communication [52].

During the test, Node1 was fixed at one end of an open street while Node2 moved away. The voice call began to experience distortion at approximately 1 km, with a throughput of around 420 Kbps. In contrast, video call performance degraded at a shorter distance, with lip-sync issues and video distortion occurring at around 800 m, corresponding to a throughput of about 700 Kbps. These results demonstrate the maximum range provided by the *WiLongH* platform in a single-hop urban LoS environment. This aligns with the requirements of WebRTC-based applications, further demonstrating the platform's capability.

Additionally, a received signal strength of approximately -96 dBm was recorded at 1 km in MCS 0 mode, optimized for low SNR environments. MCS 0 allows the system to maintain communication with low throughput, meeting the minimum SNR of 9 dB for voice and video calls. This aligns well with the theoretical link budget calculation presented in Section III-E.1, which incorporates all critical parameters, including transmit power, antenna gain, receiver sensitivity, path loss, and noise figure. Tests with a 2 MHz channel bandwidth demonstrated link loss at approximately 1.4 km when the minimum required SNR dropped to around 1–2 dB, corroborating the theoretical model. These results validate the platform's ability to sustain WebRTC-based voice and video communication over significant distances, making it a robust solution for emergency response and rural connectivity applications.

B. REAL-WORLD URBAN ENVIRONMENT EVALUATION (N-LOS)

The proposed *WiLongH* platform was tested in a real-world urban environment along Route 1 (medium range), as depicted in Fig. 9. This 300 m segment comprises a mix of large villas and open spaces, providing varied testing conditions. Node 1 was placed on a tripod in a ground-level car park, while Node 2 was strategically positioned on a rooftop to maximize coverage. Node 3 was manually moved along the route by walking, as indicated by the

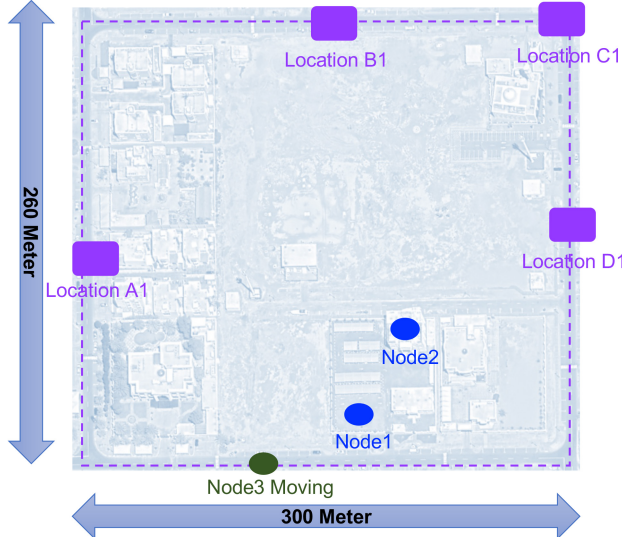


FIGURE 9. N-LoS test location along Route 1, which extends 300 m (medium range). Node 1 was placed in the car parking area, and Node 2 was positioned on the rooftop. Node 3 was manually moved by walking along the route, as shown by the dashed lines. The designated testing points were A1, B1, C1, and D1.

dashed lines. Testing points were designated at A1 (hidden by buildings), B1 (partially LoS in an open area), C1 (obstructed by buildings), and D1 (less obstructed area).

Initially, Route 1 was used to evaluate the impact of varying channel bandwidths (1 MHz and 4 MHz) on throughput and coverage, focusing on a two-node configuration. Later, a third relay node was introduced to characterize mesh performance. Throughput (UDP unicast traffic) and latency measurements were collected at these designated test locations using iPerf3 for 180 seconds [53] and the ping utility for 30 seconds, respectively. These tests were conducted both with and without the presence of the rooftop Node 2. Throughput corresponds to a 1% packet error rate. At the same time, latency was measured as the average ping over a 30-second interval at each test point, with one ping request sent per second (30 measurements per round). Both throughput and latency measurements were repeated at each test point across five rounds, and the mean values were reported to ensure reliability under changing environmental conditions. The summarized results are presented in Table 4.

Initially, without the rooftop Node 2 and using only two nodes, Node 1 in the car parking area successfully communicated with the moving Node 3 at all locations (2N-A1/B1/C1/D1) using the *WiLongH-1MHz* profile. However, with the *WiLongH-4MHz* profile, Node1's reachability to 2N-A1 (completely obscured by buildings) was compromised, with notably poor performance at 2N-C1 (behind buildings). Despite this, throughput improved at 2N-B1 (partially LoS in open space) and 2N-D1 (less shadowed area). Therefore, the 4 MHz bandwidth was deemed suboptimal in this set-up, underscoring the need for a dynamic bandwidth selection algorithm to achieve optimal performance in varying environments. Moreover, integrating additional nodes via the

TABLE 4. Real-world N-LoS test result (route 1).

Test Location	Test Profile	Throughput (Kbps)	Latency (ms)	No. of Hops
2N-A1	<i>WiLongH-1MHz</i>	797	27.1	1
2N-B1	<i>WiLongH-1MHz</i>	1397	22.7	1
2N-C1	<i>WiLongH-1MHz</i>	1130	30.2	1
2N-D1	<i>WiLongH-1MHz</i>	964	41.8	1
2N-A1	<i>WiLongH-4MHz</i>	-	-	-
2N-B1	<i>WiLongH-4MHz</i>	1854	26.7	1
2N-C1	<i>WiLongH-4MHz</i>	52	93.8	1
2N-D1	<i>WiLongH-4MHz</i>	1528	31.6	1
3N-A1	<i>WiLongH-1MHz</i>	269	60.2	2
3N-B1	<i>WiLongH-1MHz</i>	695	46	1-2
3N-C1	<i>WiLongH-1MHz</i>	486	59.4	2
3N-D1	<i>WiLongH-1MHz</i>	484	90.1	2

mesh network and adopting the *WiLongH-1MHz* profile may be necessary to enhance coverage in this test environment. When introducing a relay node on the rooftop, the results (3N-X1) showed halved throughput and doubled latency due to the *WiLongH* platform's half-duplex HaLow single-radio system. This may impact real-time voice and video call performance. According to ITU-T G.114 [54], a one-way latency below 150 ms is ideal for high-quality real-time voice communication, while values between 150–400 ms remain acceptable with minor degradation. To ensure seamless conversation quality, voice communication typically requires a minimum throughput of 200 Kbps and latency below 50 ms. For interactive video applications, a latency of less than 200 ms is recommended, with at least 1 Mbps throughput required for high-quality video transmission. This highlights the need for a multi-radio system [55] to overcome these challenges, which we plan to address in future work. Additionally, in the same route, *WiLong-LR* could not establish a link at test locations A1 and C1 with two nodes (as shown in [44, Table III]). This limitation highlights the necessity of long-range HaLow technology to cover such challenging environments. These results from the urban environment closely align with the theoretical coverage model presented earlier in Section III-E.2. The significant differences in range and performance between *WiLongH* and *WiLong-LR* stem from *WiLongH*'s use of a lower operating frequency, which results in a larger wavelength and reduced path loss. Even with similar transmission power and gains, *WiLong-LR* showed limited coverage due to its higher path loss exponent in these challenging environments. Additionally, the improved receiver sensitivity of *WiLongH* further contributes to its superior performance. The measured range and throughput outcomes confirm the model's predictions and validate the platform's capabilities in real-world urban N-LoS conditions.

Next, Route 2 (long range) encompassed a larger area of 700–800m, as shown in Fig. 10. Nodes 1 and 2 were fixed similarly to the Route 1 setup, while Node 3 was moved at

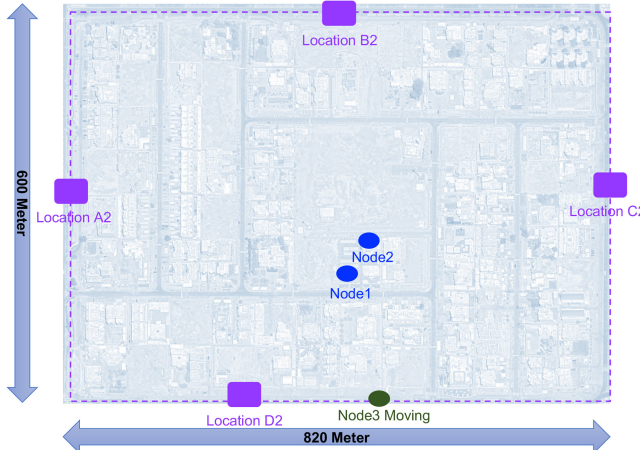


FIGURE 10. N-LoS test location along Route 2, which covers 800 m. Node 1 was in the car parking area, while Node 2 was fixed on the rooftop. The dashed lines indicated that Node 3 was moved by car along the route at 5 km/h speed. The designated testing points were A2, B2, C2, and D2.

TABLE 5. Real-world N-LoS test result (route 2: WiLongH-1MHz profile).

Test Location	Throughput (Kbps)	Latency (ms)	RSSI (dBm)	SNR (dB)	MCS
2N-A2	-	-	-95	0-1	N/A
2N-B2	781	28	-78	18	3-7
2N-C2	-	-	-96	0-1	N/A
2N-D2	191	50.9	-89	6	2-6

a controlled speed of about 5 km/h by car along the route, marked by dashed lines. To minimize signal shadowing and ensure more accurate results, the *WiLongH* platform with its antenna was mounted on a tripod positioned outside the car through the sunroof. Test points for Route 2 included A2 (hidden by buildings), B2 (partially LoS), C2, and D2 (hidden by buildings). In subsequent sections, we analyzed the voice and video call performance across these two routes. Before conducting the route-wide analysis, this initial evaluation was performed to understand the environment and the performance of the *WiLongH* profile at these designated test points.

In the subsequent evaluation phase, we replicated the experimental methodology along Route 2 with only two nodes to assess the maximum coverage provided by the long-range HaLow link. The results are summarized in Table 5. The findings revealed that despite utilizing the *WiLongH* profile and employing a 1 MHz channel bandwidth, specific points such as A2 (completely shadowed by buildings) and C2 (shadowed by buildings) exhibited no coverage. This degradation in coverage can be attributed to severe path loss, cellular interference, and challenging N-LoS conditions, as evidenced by the recorded RSSI of -95/-96 dBm and SNR of 0-1 dB, which resulted in no HaLow link. In contrast, the B2 test point demonstrated reasonable performance owing to partial LoS conditions, achieving a throughput of 781 Kbps with an RSSI of -78 dBm, SNR of 18 dB, and MCS values varying between 3 and 7. Similarly, the D2 test point

exhibited relatively better performance due to its shorter distance, achieving a throughput of 191 Kbps, an RSSI of -89 dBm, SNR of 6 dB, and MCS values between 2 and 6. These results highlight the limitations of coverage in challenging urban environments, emphasizing the importance of additional relay nodes for traffic forwarding in shadowed areas. Furthermore, the findings align with the theoretical predictions discussed in earlier sections. In comparison, *WiLong-LR* was unable to receive a signal at any of the Route 2 testing points, requiring a three-node setup with a rooftop relay node, as described in [44, Table IV]. This comparison demonstrates the strong motivation for using long-range HaLow technology in highly challenging and extended-range urban environments.

In this urban real-world environment, we evaluated the performance of continuous voice and video calls using our P2P chat application (unicast traffic) in these two routes. A Google Pixel 8 phone was tethered to the *WiLongH* platform via a USB to Ethernet converter as explained earlier. The P2P chat application, installed on the Pixel 8 phone, facilitated separate voice and video calls between the phone connected to the car parking Node 1 and the moving Node 3 (without relay Node 2). The application maintained the voice call bandwidth above 200 Kbps and the video call bandwidth above 1 Mbps for optimal performance. Like the previous exercise, in Route 1, we studied the impact *WiLongH* profile with 1 MHz and 4 MHz channel bandwidth with two nodes in voice and video call performance, later in Route 2 with only 1 MHz. The results of the voice and video calls along Route 1, utilizing the *WiLongH* profile with a 1 and 4 MHz channel bandwidth with two nodes, are depicted in Fig. 11.

The voice and video call requirements were not consistently met in certain areas, with only 64% voice and 30% video call coverage observed in this route with 1 MHz channel bandwidth (Fig. 11: (a)). However, upon using 4 MHz channel bandwidth, numerous areas exhibited non-functional voice or video calls due to reduced signal quality (Fig. 11: (b)), although overall video call coverage improved owing to the higher bandwidth, achieving 41% voice or 34% video call coverage.

In Route 2, we evaluated voice and video call performance similarly with the same two nodes, utilizing the *WiLongH* profile with a 1 MHz channel bandwidth. The results are depicted in Fig. 11: (c). Unlike Route 1, voice and video calls exhibited functionality only in specific areas along Route 2, achieving only 18% voice or 7% video call coverage. This disparity aligns with our previous findings of pronounced path loss and coverage challenges in the designated test locations. The corresponding signal strength analysis confirms and reinforces the above observation. Poor RSSI (Received Signal Strength Indicator) values (less than -95 dBm) have been concealed for clarity. Notably, in both Route 1 and Route 2 results, voice call performance was relatively better, owing to the application's lower bandwidth requirements compared to video calls. When comparing

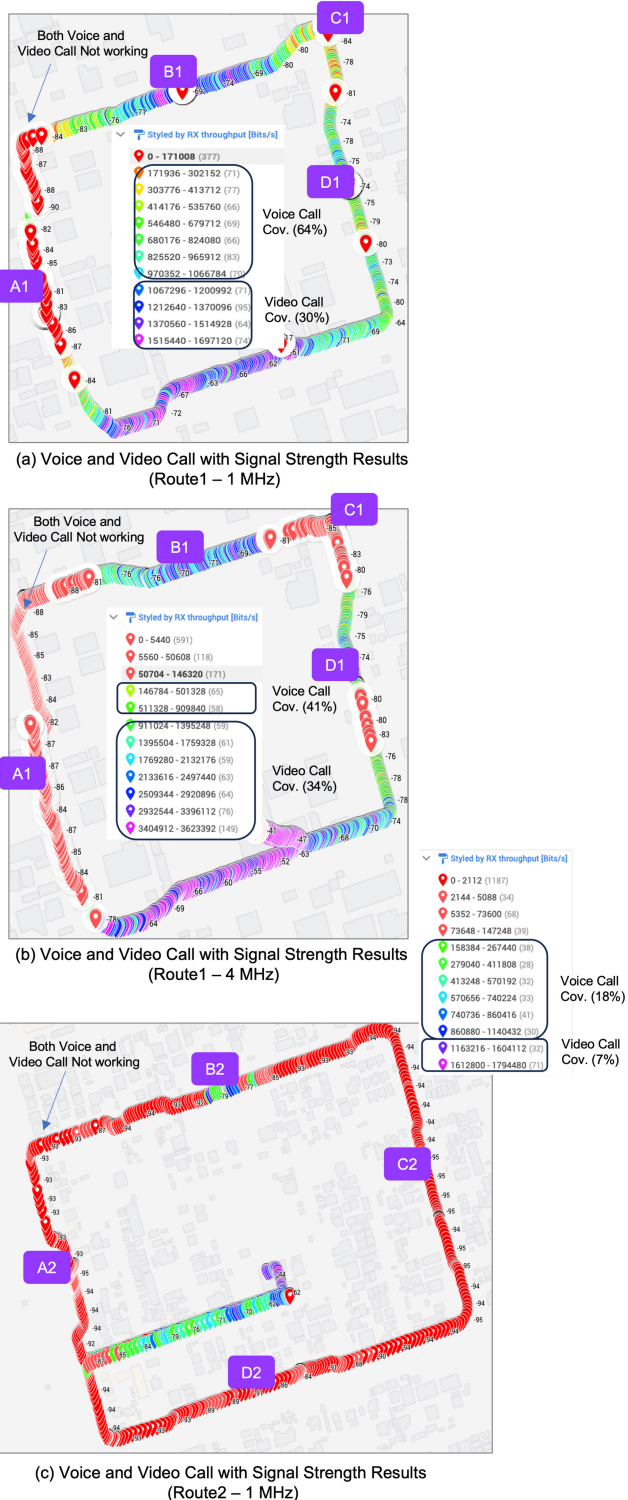


FIGURE 11. Voice and video call performance with signal strength results (two nodes): (a) Route 1 with 1 MHz channel bandwidth (CBW), (b) Route 1 with 4 MHz CBW, (c) Route 2 with 1 MHz CBW. The figures indicate the percentage of bandwidth requirements met for both voice and video calls, with areas where both audio and video fail marked in red.

the same voice and video call performance with *WiLong-LR* along these routes, *WiLong-LR* performed poorly in Route 1, even with two nodes, and worked only near the

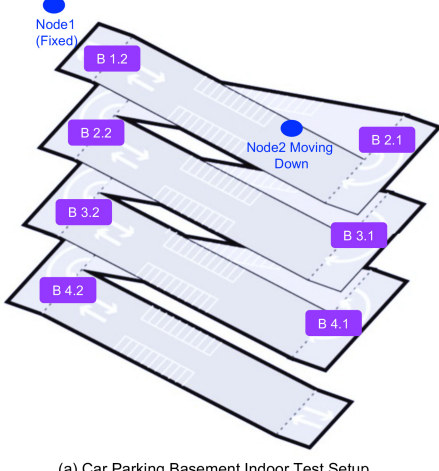
car parking Node 1 and around location B1. Due to the lack of performance in Route 1, further comparisons in Route 2 were not pursued with *WiLong-LR*. Instead, a three-node setup with a rooftop relay node was used, as shown in [44, Figs. 9 and 11]. Hence, this evaluation of voice and video call performance in an urban environment underscores the importance of using long-range HaLow radio and increasing the number of nodes in the mesh along these routes. Additionally, implementing dynamic bandwidth selection and multi-radio support, which we plan to address in future work, is crucial.

C. INDOOR: MULTI-FLOOR RESULTS

In this section, we aimed to compare the performance of the *WiLongH* platform with that of *WiLong-LR* in a basement car parking area using a two-node setup. This environment presents significant challenges for wireless signal propagation due to physical obstructions, multipath interference, environmental conditions, and vehicle interference. As depicted in Fig. 12: (a), Node 1 was fixed at B 1.2 on a tripod, while Node 2 was moved downward through the parking area by walking. The closer downward test points included B 2.2, 3.2, and 4.2, whereas B 2.1, 3.1, and 4.1 were comparatively farther from Node 1. Throughput (unicast traffic), latency, and signal strength measurements were taken at these designated test points, with traffic sent from Node 1 to Node 2 in five different rounds as explained in the previous section.

As shown in Fig. 12: (b), although *WiLong-LR* operating at 2.4 GHz can penetrate two floors down at direct downward points (reaching B 3.2), it struggles at farther test points, only reaching B 2.1, which is less than one floor down. In contrast, *WiLongH* successfully penetrates three floors down at near points with reliable throughput, latency, and RSSI and maintains a stable connection at far points up to B 3.1 (two floors down). To analyze and correlate these *WiLongH* results, Fig. 12: (c) clearly illustrates the corresponding Rx throughput and SNR variations as Node 2 moves downward. For example, at nearby test points (directly downward), the SNR is around 20-25 dB with more than 600 Kbps Rx throughput. However, at farther test points, the SNR is around 5-7 dB at B 2.1 and B 3.1 with reasonable Rx throughput, though no link was established at B 4.1. These results highlight the *WiLongH* platform's superior capability in addressing the challenges of an indoor basement car parking environment for long-range HaLow mesh networks. This analysis further reinforces the necessity of a HaLow mesh system in scenarios where first responder use cases may demand coverage beyond five floors.

Moreover, at 5 GHz ([44, Fig. 14]), no links were established at any test points. These results from the basement parking environment align precisely with the theoretical coverage range modeling discussed in Section III-E.2, demonstrating the impact of a higher path loss exponent in this challenging environment. The superior performance of sub-1 GHz frequencies over 2.4/5 GHz and the better



(a) Car Parking Basement Indoor Test Setup

Location	WiLong-LR-2442			WiLongH		
	Throughput (Kbps)	Latency (ms)	RSSI (dBm)	Throughput (Kbps)	Latency (ms)	RSSI (dBm)
B 2.1	3340	13.1	-73	44	63.5	-89
B 2.2	14500	5.6	-57	955	67	-61
B 3.1	Not Reachable			40	225	-95
B 3.2	4050	6.7	-74	727	28.9	-77
B 4.1	Not Reachable			Not Reachable		
B 4.2	Not Reachable			637	31.6	-83

(b) Car Parking Basement Indoor Test Results (Throughput, Latency and RSSI)

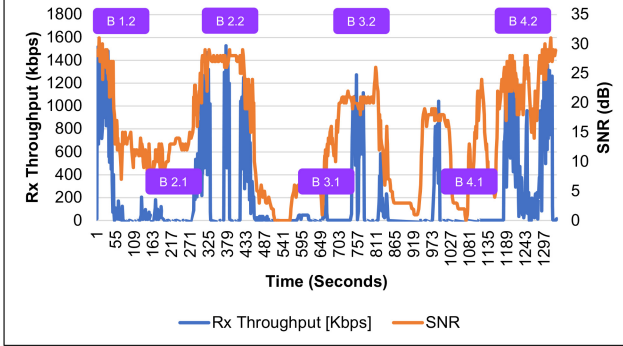


FIGURE 12. Car parking basement indoor test setup & results: (a) Node 1 was stationed in basement 1 while Node 2 traversed basement levels 2 through 4 on foot. (b) Throughput, latency, and RSSI were measured at various positions using the WiLong-LR-2442 and WiLongH profiles. (c) Correlation between throughput and SNR in a time series analysis with WiLongH profiles.

receiver sensitivity of WiLongH, even with similar or higher transmission power in WiLong-LR, are critical to achieving extended connectivity.

D. MULTICAST & MULTI-HOP (MCMH) AUDIO CALL PERFORMANCE ANALYSIS

Multicast audio is a crucial application in first responder networks with H2H communication, particularly for group calls and public announcements. This subsection analyzes the performance of multicast audio calls within the WiLongH

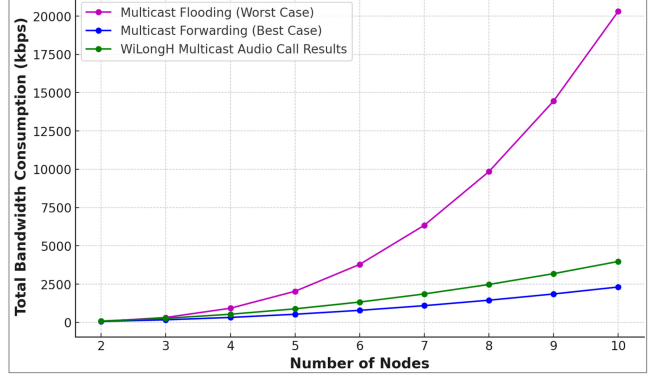


FIGURE 13. Multicast audio call results at desk: The WiLongH multicast audio call performance on par with the best-case scenario (multicast forwarding), significantly outperforming the worst-case scenario (multicast flooding). The analysis spans network sizes from 2 to 10 nodes, showcasing the scalability and efficiency of the WiLongH platform.

platform, focusing on bandwidth consumption patterns across different multicast strategies and the implications of mesh network scalability.

1) MULTICAST AUDIO CALL ANALYSIS AT DESK

Two primary multicast strategies were evaluated in this study:

- *Multicast Flooding*: Each node that receives a multicast packet forwards it to all its neighbors except the one from which the packet was received. While this approach ensures high reliability, it consumes substantial bandwidth due to the large number of redundant transmissions.
- *Multicast Forwarding*: A more efficient approach that selectively forwards multicast packets along the network's minimum spanning tree (MST). By reducing redundant transmissions, this strategy significantly decreases bandwidth consumption.

The overall bandwidth consumption for each strategy was analyzed using the following equations when all the mesh nodes are transmitting:

$$B_{\text{flooding}} = n \times [(n - 1)^2 \times b + C] \quad (10)$$

$$B_{\text{forwarding}} = n \times [(n - 1) \times b + C] \quad (11)$$

where:

- n is the number of nodes,
- b is the bandwidth per audio stream (25 kbps),
- C is the overhead from batman-adv management messages (6 kbps).

A practical evaluation was conducted using a UDP multicast audio application developed with GStreamer [56] and optimized using batman-adv multicast extensions [57]. This evaluation tested the WiLongH platform with 2–10 nodes and compared the results with the theoretical models. The findings, illustrated in Fig. 13, show the total bandwidth consumption (in Kbps) as the number of mesh nodes increases from 2 to 10.

The results highlight a significant difference in bandwidth consumption as the network scales, particularly in multi-hop communication from 3 to 10 nodes, depending on the topology. The *WiLongH* multicast solution shows bandwidth consumption on par with multicast forwarding for up to 5 mesh nodes. For 10 nodes, multicast forwarding requires only 2.5 Mbps, which is feasible within a HaLow mesh network using a reasonable MCS (e.g., MCS 2). In contrast, multicast flooding exceeds 20 Mbps, making it impractical and adversely affecting mesh scalability.

The practical results also reveal discrepancies between theoretical models and real-world performance due to factors such as signal interference, packet loss, and dynamic topology. Future work will focus on refining the multicast algorithm to reduce overhead and improve scalability. Adaptive multicast strategies that dynamically switch between flooding and forwarding based on real-time network conditions may provide an optimal balance between reliability and efficiency.

2) MCMH AUDIO CALL PERFORMANCE IN OUTDOOR URBAN ENVIRONMENT

An outdoor experiment was conducted to assess the performance of multicast audio calls using the *WiLongH* platform as mentioned previously, with four nodes placed in a car parking area near an office, as shown in Fig. 14: (a). The nodes were arranged in a rectangular formation, with multicast audio calls initiated across all mesh nodes from a starting point, and performance analyses conducted at designated locations. Signal strength between nodes and throughput during multicast audio calls were evaluated.

For this experiment, we attached a clip to the back cover of the *WiLongH* platform to assess two positioning setups:

- The *hand-held clip position*, where the clip was held at around head height, away from the body to simulate a free-space environment.
- The *belt clip position*, where the clip was attached to the belt, at a lower height and close to the body, introducing body shadowing effects.

As shown in Fig. 14: (b), a notable RSSI difference of 4-7 dB was observed from Node C to the other nodes. In the hand-held clip position, this RSSI improvement enabled all four audio streams to function concurrently. However, in the belt clip position, audio communication was limited to one or two streams. Fig. 14: (c) further shows that although four audio call streams consumed similar average Tx and Rx throughput in the hand-held clip position compared to only two streams in the belt clip position, data consumption did not double. This is attributed to the improved link quality in the free-space position, which reduced packet error rates and enhanced mesh forwarding.

3) MCMH AUDIO CALL PERFORMANCE IN INDOOR ENVIRONMENT

We conducted a similar exercise in a challenging indoor office setup, as shown in Fig. 15 (a). Nodes 1 to 3 were

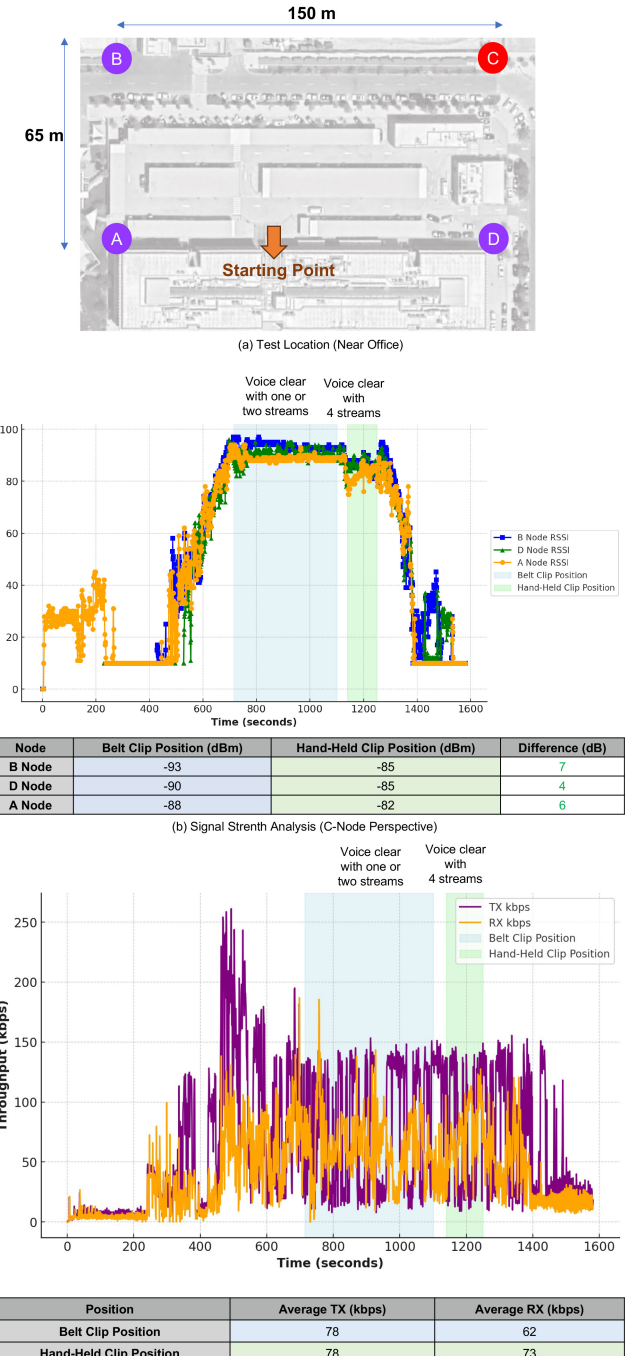


FIGURE 14. MCMH audio call performance results in an outdoor urban environment.
(a) Test location near the office with four nodes. (b) Signal strength from the perspective of C-node with other nodes. (c) Throughput analysis at C-node comparing the hand-held clip position and belt clip position.

placed in a linear topology along an office corridor on the ground floor, with the 4th node positioned on the first floor to evaluate the *WiLongH* platform's performance in an indoor environment. The results show a signal strength improvement of 5-8 dB in the hand-held clip position compared to the belt clip position, as illustrated in Fig. 15 (b). This improvement enabled two audio streams to function in the hand-held clip position, whereas in the belt clip position, only one node's

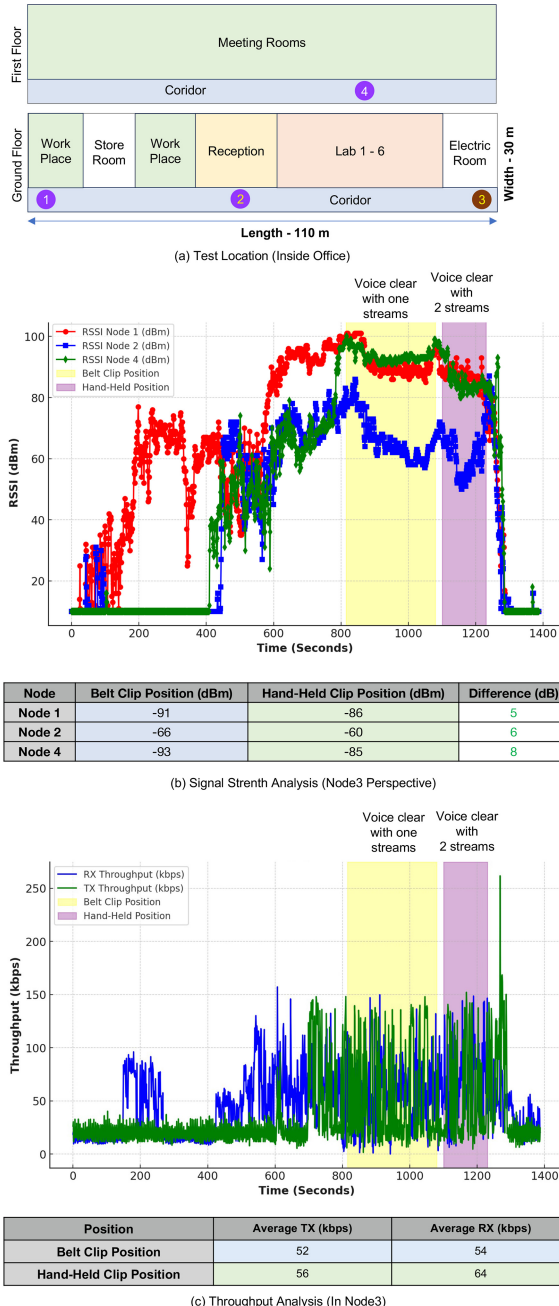


FIGURE 15. MCMH audio call performance results in an indoor environment. (a) Test location inside an office with 4 nodes. (b) Signal strength from Node 3's perspective with other nodes. (c) Throughput analysis at Node 3, comparing hand-held clip position and belt clip positions.

audio call was operational, limiting communication to one person speaking at a time.

Additionally, throughput analysis, as indicated in Fig. 15 (c), shows that the hand-held clip position achieved similar Tx/Rx throughput for two audio streams, while the belt clip position only supported a single stream. This outcome highlights the platform's effectiveness in handling multicast multi-hop audio calls across different environments, with the

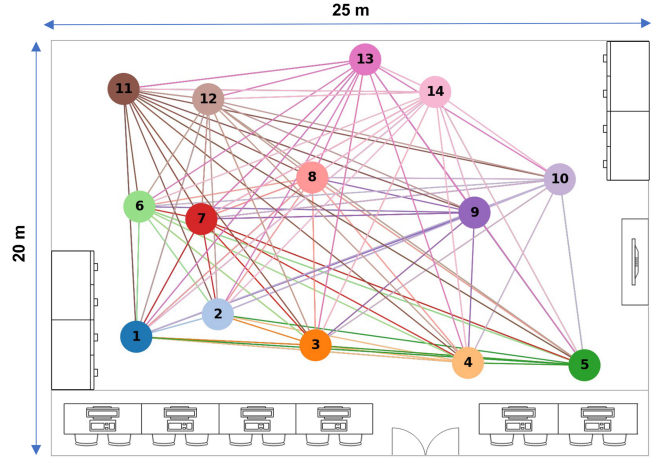


FIGURE 16. Dense mesh network setup & topology in indoor arena (20m x 25m): fourteen WiLongH nodes deployed at random positions. Full mesh network topology formed, with each node connecting to 13 neighbors.

hand-held clip position proving more advantageous in signal quality and network performance.

E. DENSE MESH NETWORK RESULTS (INDOOR)

To evaluate the scalability of the WiLongH platform in a dense mesh network, we experimented in an indoor arena measuring approximately 25 m in length and 20 m in width, as shown in Fig. 16. In this setup, we randomly placed 14 WiLongH nodes, forming a full mesh topology where each node interacted with all 13 other nodes as neighbors. Due to the relatively small area of the indoor environment, we reduced the transmission power to 14 dBm to optimize coverage and channel reuse. This setup simulates a smaller-scale version of practical real-time deployments for first responder scenarios in H2H communication, which could involve a similar topology over a larger area, potentially covering 2-3 km with multiple interacting nodes. We evaluated three distinct traffic scenarios: (a) One-to-Many (1-M), (b) Many-to-One (M-1), and (c) One-to-One (1-1) [Paired].

The One-to-Many (1-M) scenario was developed to evaluate the broadcast and multicast capabilities of the HaLow mesh network, particularly useful for first responder situations where critical data from a drone or hand-held device must be disseminated to all nodes. In this experiment, an iPerf3 client on a single device transmitted TCP packets concurrently to 13 nodes acting as iPerf3 servers for one hour. The resulting throughput distributions, shown in Fig. 17 (a), reveal a median throughput below 0.15 Mbps across most nodes, with slight variability in the interquartile range (IQR). The presence of outliers suggests occasional spikes or drops, likely due to transient network conditions, interference, or TCP slow start. As mentioned earlier, the GW16146 radio data rate is limited to 4 Mbps overall, although the SX-NEWAH module inside this radio supports up to 15 Mbps. With the actual module in future deployments, this median throughput could increase to 600 Kbps per node, making it ideal for voice, low-quality video, and broadcast/multicast services.

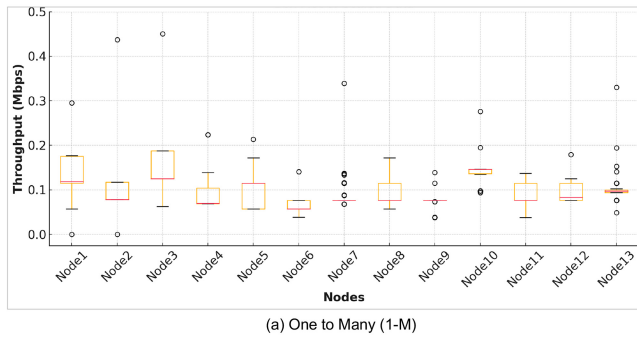


FIGURE 17. Dense mesh results: box plot comparison on TCP throughput, (a) One-to-Many (1-M), (b) Many-to-One (M-1), and (c) One-to-One (1-1) [Paired].

The Many-to-One (M-1) scenario was designed to assess the HaLow mesh network's capacity for aggregating data from multiple nodes, particularly relevant for first responder operations where the Flight Mission Operation (FMO) collects video streams from drones and hand-held devices. In this setup, 13 nodes acted as iPerf3 clients, transmitting TCP packets (unicast traffic) to a primary node configured as an iPerf3 server with multiple ports for one hour. As shown in Fig. 17 (b), the results reveal median throughput values below 0.2 Mbps, with zero-byte throughput instances attributed to contention among the 13 nodes competing for single-channel access. The observed variability in IQR and outliers underscores the challenges of CSMA/CA contention, highlighting the need for multi-radio or multi-channel systems to mitigate concurrency issues in multi-hop mesh networks. With the SX-NEWAH module, each node could achieve 800 Kbps, enabling medium-quality video streams in the FMO scenario. In practical deployments, it is unlikely that all 13 drones would transmit video streams simultaneously; typically, 2-3 drones from critical areas

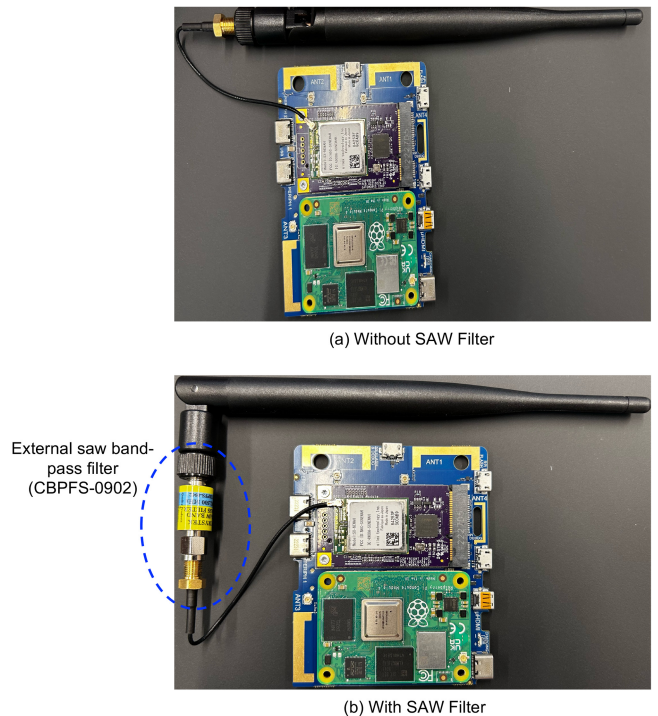


FIGURE 18. Cellular interference analysis setup: (a) Without SAW filter between HaLow module and antenna, (b) With external SAW filter added between HaLow module and antenna.

would send streams while all 13 drones in mission, resulting in approximately 2.4 Mbps per drone.

The One-to-One (1-1 paired) scenario evaluates direct communication between paired nodes in the HaLow mesh network, relevant for first responder situations where users, such as doctors or police officers, need to communicate directly. In this setup, each of the 7 pairs comprised an iPerf3 server and an iPerf3 client, transmitting TCP packets (unicast traffic) concurrently for one hour. As depicted in Fig. 17: (c), the throughput distribution reveals median throughput values below 0.5 Mbps, almost double the previous 1-M and M-1 scenarios, due to fewer nodes contending for channel access. Variability in the interquartile range (IQR) and the presence of outliers indicate differences in throughput stability, highlighting the influence of transient network conditions or TCP slow start. Similarly, with the SX-NEWAH module, per-pair bandwidth could increase to 2 Mbps, ideal for voice and video communication in each pair. Hence, our *WiLongH* platform has proven scalable and capable of meeting the requirements of practical first responder use cases at the ground level. In future work, we aim to evaluate the dense mesh network with 14 nodes over a 2-3 km range in urban areas to analyze obstacles (N-LoS propagation), interference, Fresnel zone impacts, and mobility scenarios.

F. CELLULAR INTERFERENCE ANALYSIS

In the *WiLongH* platform deployment, particularly in the US band (902-928 MHz), there is overlap with licensed cellular

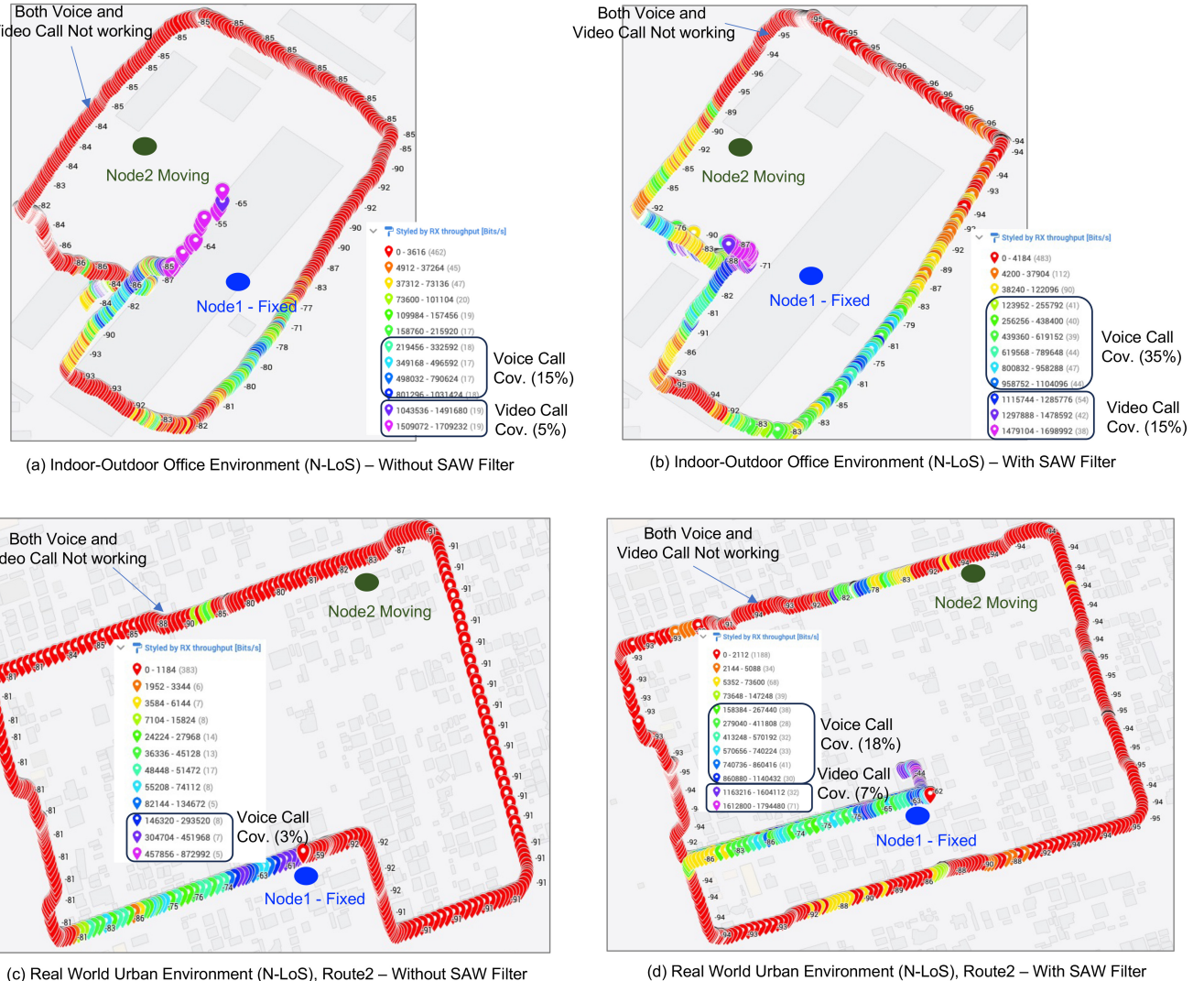


FIGURE 19. Cellular interference analysis with HaLow Mesh (US band: 902-928 MHz) results: (a) Indoor-Outdoor office without SAW filter, (b) Indoor-Outdoor office with SAW filter. Node 1 was fixed inside the office, and Node 2 moved around the office by walking. (c) Route 2 without SAW filter, and (d) Route 2 with SAW filter. Node 1 was fixed in a car parking area, and Node 2 moved along Route 2 in a car at 5 km/h. Voice and video call improvement with the SAW filter is presented.

bands in many countries [58]. For example, this band is used for International Mobile Telecommunications (IMT) in the UAE [59], [60]. This overlap can impact performance due to interference from cellular traffic with the long-range HaLow mesh network. Therefore, it is essential to analyze these effects and explore mitigation strategies. To address this, we implemented a setup with and without an external SAW filter, as shown in Fig. 18. The filter was placed between the HaLow module and the external antenna. We analyzed cellular interference on voice and video call performance (unicast traffic) in two scenarios: near an office and along Route 2, as previously described in Fig. 10. In the office setup, Node 1 was placed on a table indoors, while Node 2 was initially positioned indoors and then moved outside around the building by walking. For Route 2, Node 1 was fixed in a car parking area, and Node 2 moved by car at a controlled speed of 5 km/h, with the *WiLongH* platform and antenna positioned outside the car's sunroof,

as explained earlier, to avoid signal shadowing and improve results through higher antenna placement.

Comparing Fig. 19 (a) and (b), the addition of the SAW filter resulted in a 20% improvement in voice call and a 10% improvement in video call coverage in the indoor-outdoor office space. Additionally, we observed an overall improvement in signal quality and fewer areas where voice or video calls failed compared to earlier results without the filter. Similar observations were made along Route 2, Fig. 19 (c) and (d), where voice call coverage improved by 15% and video call coverage improved by 7% with the SAW filter. Thus, the SAW filter enhances overall performance and long-range link quality while reducing the noise floor.

Even though the SAW filter improves *WiLongH* performance in the presence of cellular interference, it results in a 4.8 dB loss in the overall link margin between two nodes. These findings emphasize the importance of designing the *WiLongH* platform with a customized EU band

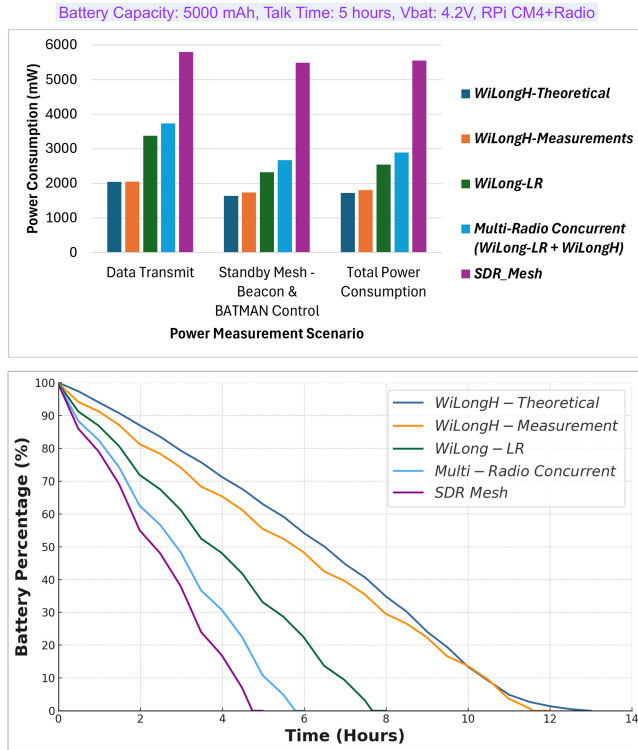


FIGURE 20. Power consumption analysis: (upper) total power consumption during active data transmission and standby mesh states for *WiLong-LR*, *WiLongH*, multi-radio concurrent (*WiLong-LR* + *WiLongH*), and SDR Mesh. (lower) battery depletion over time for different platforms. Battery life is improved by 33% using the *WiLongH* platform compared to *WiLong-LR*.

(863–868 MHz), which is unlicensed in the UAE, for future deployment with sufficient Telecommunications and Digital Government Regulatory Authority (TDRA) approval. This approach maintains similar Tx power, channel bandwidth, and duty cycle, but eliminates the need for a filter.

G. POWER CONSUMPTION ANALYSIS

The 802.11ah (HaLow) standard is optimized for energy efficiency, making the power consumption of the *WiLongH* platform a key focus of this study. For this analysis, we used a 5000 mAh battery at a platform voltage of 4.2V. Power consumption was measured in milliwatts (mW) under three conditions: active data transmission, standby mesh (only transmitting mesh beacons and batman-adv control messages), and total power consumption over 5 hours of the talk time in a day. As shown in Fig. 20: Upper, the *WiLongH* platform demonstrates a 33% reduction in power consumption during active transmission, a 29% reduction in standby mesh states, and a 20% overall reduction compared to the *WiLong-LR* platform. Fig. 20: Lower illustrates battery depletion over time across various platforms using alternating 30-minute cycles of active talk time and standby mesh states, with the *WiLongH* platform exhibiting a 33% increase in battery life, lasting 12 hours compared to 8 hours for the *WiLong-LR* platform. This aligns with the theoretical energy efficiency model discussed in Section III-E.4, demonstrating

the *WiLongH* platform's reduced energy per bit compared to *WiLong-LR*, leading to improved efficiency during both transmission and standby states. The battery depletion trends are illustrated in Fig. 20.

Additionally, two other scenarios were evaluated: one with a commercial SDR (Software Defined Radio) mesh solution [61] and another using a multi-radio (MR) concurrent solution combining both *WiLongH* and *WiLong-LR* radios. In these cases, battery life was reduced to 5 hours for the SDR mesh and 6 hours for the MR solution. Thus, while the *WiLongH* platform is highly power efficient, integrating additional radios significantly impacts overall power consumption, which must be carefully considered in multi-radio configurations. While our primary focus was to compare power consumption across different operations in a mesh topology using various radios (Wi-Fi, HaLow, SDR, and Multi-Radio configurations), we also analyzed HaLow in infrastructure mode (Access Point and Station mode) compared to mesh mode. The findings reveal that infrastructure mode consumes approximately 15–17% less power than mesh mode. This reduction is attributed to the decreased overhead in infrastructure mode, as it avoids the periodic batman-adv control message exchanges (default Originator Message (OGM) interval of 1 second), routing table computations, and frequent neighbor discovery associated with 802.11s mesh networks.

Table 6 provides a comprehensive summary of the performance evaluation, highlighting key observations, identified challenges, and directions for future work.

V. CONCLUSION

To address the critical demands of ground-based H2H communication deployments, we developed the *WiLongH* platform, enabling on-demand long-range Wi-Fi HaLow mesh networks. The platform leverages commercial off-the-shelf hardware and open-source software, integrating the 802.11s mesh link with the batman-adv and optimized radio profiles supported by an analytical model. Our LoS evaluations demonstrated the platform's capabilities, supporting voice calls over 1 km with 420 Kbps throughput and video calls up to 800 m with 700 Kbps throughput. Real-world urban environment evaluations showed a success rate of 64% for voice calls and 30% for video calls over routes of 300 m to 700 m with a 1 MHz channel bandwidth, highlighting the need for increased mesh node density. Additionally, the *WiLongH* platform delivered reliable throughput, latency, and RSSI performance across multi-floor environments, including RF-challenging basement scenarios. Multicast and multi-hop audio call tests demonstrated practical results with efficient multicast forwarding, achieving a 4–8 dB improvement and stable throughput with 4 nodes in both indoor and outdoor environments. The platform's scalability was confirmed in dense mesh configurations with 14 nodes, and the use of a SAW filter in the US band (902–928 MHz) effectively mitigated cellular interference, improving voice call performance by 20% and video calls by 10%. Furthermore,

TABLE 6. Comprehensive insights from performance evaluations.

Sec.	Evaluation Scenario	Key Observations	Identified Challenges	Significance and Future Work
4B	Real-World Urban Environment Evaluation (N-LoS)	Reliable communication at Route 1 and partially LoS points in Route 2. <i>WiLongH</i> outperformed <i>WiLong-LR</i> in urban N-LoS conditions.	Heavily shadowed points and increased latency with relay nodes. 4 MHz bandwidth underperformed in multipath environments.	Highlights the need for dynamic bandwidth selection, additional nodes, and multi-radio systems for scalability.
4C	Indoor: Multi-Floor Results	<i>WiLongH</i> achieved stable connectivity over three floors at near points and two floors at far points. SNR improved up to 25 dB for direct downward points.	No connection at the farthest point (B 4.1). Performance degraded due to multipath and shadowing.	Confirms <i>WiLongH</i> 's superiority in indoor settings. Future work includes evaluating mobility across multi-floor environments.
4D	Multicast & Multi-hop Audio Call Performance	<i>WiLongH</i> multicast solution on par with multicast forwarding achieved scalability with 2.5 Mbps for 10 nodes. Hand-held clip positions improved RSSI and supported multiple audio streams.	Multicast flooding exceeded 20 Mbps, reducing scalability. Belt clip positions suffered from poor RSSI and limited audio communication.	Future work focuses on adaptive strategies and optimizing performance for body-shadowing scenarios.
4E	Dense Mesh Network Results (Indoor)	Reliable paired node communication (up to 0.5 Mbps). Feasibility of 2-3 simultaneous video streams in drone operations with SX-NEWAH.	Contention challenges in Many-to-One (0.2 Mbps) and One-to-Many (0.15 Mbps). GW16146 Hardware limitations constrained throughput.	Plans to explore optimized contention strategies, mobility scenarios, and multi-radio designs for dense networks.
4F	Cellular Interference Analysis	SAW filter improved voice and video bandwidth by 20% and 10% (office) and 15% and 7% (Route 2).	SAW filter reduced link margin by 4.8 dB. Cellular interference degraded signal quality.	Transitioning to unlicensed EU bands (863-868 MHz) is proposed to eliminate filter dependency.
4G	Power Consumption Analysis	33% reduction in active transmission power. 29% reduction in standby states. Improved battery life (12 hours vs. 8 hours for <i>WiLong-LR</i>). The practical results closely align with theoretical predictions, validating the proposed energy efficiency model.	Multi-radio or SDR setups significantly reduced battery life to 5-6 hours. Hardware-level inefficiencies, such as additional power draw from the RPi-based host system, limit the battery life compared to theoretical estimates.	Plans to integrate multi-radio with optimized protocols for further energy savings.

the platform achieved a 33% improvement in battery life compared to traditional long-range Wi-Fi mesh systems.

VI. FUTURE WORK

Our evaluation emphasizes the need for a dynamic bandwidth selection algorithm to optimize the trade-offs between range and throughput, particularly when using a 4 MHz channel bandwidth in areas with fluctuating signal-to-noise ratios (SNR). The half-duplex nature of HaLow radios, which halves throughput and doubles latency with each mesh hop, underscores the necessity of a multi-radio system to enhance performance over extended routes while incorporating optimized energy-saving mechanisms. Future work will include the development of adaptive multicast strategies to balance reliability and efficiency, while also mitigating body shadowing effects in various deployment scenarios. Additionally, integrating the SX-NEWAH module will leverage its advantages in throughput and latency, enabling further experimentation in urban environments with 14 or more nodes to strengthen the scalability and robustness of the *WiLongH* platform. Transitioning to a customized EU-band module (863-868 MHz) will also

enhance performance by eliminating the need for filters and reducing cellular interference, particularly in high-density deployment scenarios. To further extend the capabilities of the *WiLongH* platform, we plan to develop a digital twin framework, enabling emulation and Mininet-WiFi-based simulations. This tool will be made available to the research community, fostering collaborative research and accelerating advancements in long-range HaLow mesh networks.

ACKNOWLEDGMENT

The authors thank Jean-Pierre Giacalone, Dr. Monika Prakash, Dr. Michael Baddeley, Mr. Petri Mäntylä, Mr. Riku Koskinen, and Mika Joenperä from the Technology Innovation Institute, UAE, for their valuable discussions and insightful suggestions.

REFERENCES

- [1] IEEE Standard for Information Technology—Telecommunications and Information Exchange Between Systems—Local and Metropolitan Area Networks—Specific Requirements—Part 11: Wireless LAN Medium Access Control (MAC) and Physical Layer (PHY) Specifications, IEEE Standard 802.11-2020 (Revision of IEEE Std 802.11-2016), 2021.

- [2] "Wi-Fi alliance® celebrates 25 years of Wi-Fi® innovation and impact," Accessed: Sep. 28, 2024. [Online]. Available: <https://www.wi-fi.org/news-events/newsroom/wi-fi-alliance-celebrates-25-years-of-wi-fi-innovation-and-impact>
- [3] *IEEE Standard for Information Technology—Telecommunications and Information Exchange Between Systems—Local and Metropolitan Area Networks—Specific Requirements—Part 11: Wireless LAN Medium Access Control (MAC) and Physical Layer (PHY) Specifications Amendment 2: Sub 1 GHz License Exempt Operation*, IEEE Standard 802.11ah-2016 (Amendment to IEEE Std 802.11-2016, as amended by IEEE Std 802.11ai-2016), 2017.
- [4] "How to get the best out of mesh WiFi @ home," Accessed: Sep. 28, 2024. [Online]. Available: https://www.wifi-ks.org/_files/ugd/4b9f8f_30a7b892129f46b59757fd6c3af16f58.pdf
- [5] T. Sanquist, B. Brisbois, and M. Baicum, "Attention and situational awareness in first responder operations," Pacific Northwest Nat. Lab., Alexandria, VA, USA, Rep. PNNL-25158, 2016.
- [6] R. Akeela and Y. Elziq, "Design and verification of IEEE 802.11 ah for IoT and M2M applications," in *Proc. IEEE Int. Conf. Pervasive Comput. Commun. Workshops (PerCom Workshops)*, 2017, pp. 491–496.
- [7] M. Bembe, A. Abu-Mahfouz, M. Masonta, and T. Ngqondi, "A survey on low-power wide area networks for IoT applications," *Telecommun. Syst.*, vol. 71, pp. 249–274, Mar. 2019.
- [8] M. Alam, N. Ahmed, R. Matam, and F. A. Barbuiya, "Analyzing the suitability of IEEE 802.11ah for next generation Internet of Things: A comparative study," *Ad Hoc Netw.*, vol. 156, Apr. 2024, Art. no. 103437.
- [9] H. D. Hristov, *Fresnel Zones in Wireless Links, Zone Plate Lenses and Antennas*. Norwood, MA, USA: Artech House, Inc., 2000.
- [10] "Fresnel zone calculator," Accessed: Oct. 28, 2024. [Online]. Available: <https://afar.net/fresnel-zone-calculator/>
- [11] S. Tschimben, K. Gifford, and R. Brown, "IEEE 802.11ah SDR implementation and range evaluation," in *Proc. IEEE Wireless Commun. Netw. Conf. (WCNC)*, 2019, pp. 1–6.
- [12] Y. Liang and S. Midkiff, "Multipath fresnel zone routing for wireless ad hoc networks," in *Proc. IEEE Wireless Commun. Netw. Conf.*, vol. 4, 2005, pp. 1958–1963.
- [13] I. W. Mureithi, "Extending IEEE 802.11 (Wi-Fi) range: Experimental validation and fundamental performance limits determination," Ph.D. dissertation, Jomo Kenyatta Univ. Agr. Technol., Pan African Univ. Inst. Basic Sci. Technol. Innov., Juja, Kenya, 2018.
- [14] "Proposed IEEE 802.11ah use cases," IEEE 802.11 Working Group, 2011. Accessed: Oct. 28, 2024. [Online]. Available: <https://mentor.ieee.org/802.11/dcn/11/11-11-0017-00-00ah-proposed-ieee-802-11ah-use-cases.pdf>
- [15] S. Aust, "Measurement study of IEEE 802.11 ah sub-1 GHz wireless channel performance," in *Proc. IEEE 21st Consum. Commun. Netw. Conf. (CCNC)*, 2024, pp. 847–850.
- [16] B. S. Pavan and V. Harigovindan, "Deep learning based optimal restricted access window mechanism for performance enhancement of IEEE 802.11ah dense IoT networks," *Telecommun. Syst.*, vol. 87, pp. 1–14, Sep. 2024.
- [17] U. Sangeetha, K. Babu, S. Saritha, and K. Preetha, "An energy efficiency optimization for uplink communication in IEEE 802.11ah under restricted access window," *Wireless Pers. Commun.*, vol. 138, pp. 799–815, Aug. 2024.
- [18] S. M. Soares and M. M. Carvalho, "Impact of Rayleigh fading channel on IEEE 802.11ah networks under restricted access window mechanism," in *Proc. 19th Int. Symp. Wireless Communication Syst. (ISWCS)*, 2024, pp. 1–6.
- [19] A. Jamali, B. S. Ghahfarokhi, and M. Abedini, "Improving performance of association control in IEEE 802.11ah-based massive IoT networks," *IEEE Internet Things J.*, vol. 9, no. 11, pp. 8572–8583, Jun. 2022.
- [20] L. Tian, S. Santi, A. Seferagić, J. Lan, and J. Famaey, "Wi-Fi HaLow for the Internet of Things: An up-to-date survey on IEEE 802.11ah research," *J. Netw. Comput. Appl.*, vol. 182, May 2021, Art. no. 103036.
- [21] I. K. A. Enriko and F. N. Gustiyana, "Wi-Fi HaLow: Literature review about potential use of technology in agriculture and smart cities in Indonesia," in *Proc. Int. Conf. Green Energy, Comput. Sustain. Technol. (GECOST)*, 2024, pp. 277–281.
- [22] S. Maudet, G. Andrieux, R. Chevillon, and J.-F. Diouris, "Practical evaluation of Wi-Fi HaLow performance," *Internet Things*, Dec. 2023, Art. no. 100957.
- [23] S. Maudet, G. Andrieux, R. Chevillon, and J.-F. Diouris, "Evaluation and analysis of the Wi-Fi HaLow energy consumption," *IEEE Internet Things J.*, vol. 11, no. 17, pp. 28244–28252, Sep. 2024.
- [24] M. A. Fayyaz, "Networking capabilities of IEEE 802.11s and IEEE 802.11ah systems," M.S. thesis, Faculty Comput. Electr. Eng., Tampere Univ. Technol., Tampere, Finland, 2016.
- [25] N. M. Anas et al., "Performance analysis of outdoor wireless mesh network using BATMAN advanced," in *Proc. IEEE/ACIS 16th Int. Conf. Softw. Eng., Artif. Intell., Netw. Parallel/Distrib. Comput. (SNPD)*, 2015, pp. 1–4.
- [26] U. Ashraf et al., "WiMesh: Leveraging mesh networking for disaster communication in poor regions of the world," 2021, *arXiv:2101.00573*.
- [27] S. Unni et al., "Performance measurement and analysis of long range Wi-Fi network for over-the-sea communication," in *Proc. 13th Int. Symp. Model. Optim. Mobile, Ad Hoc, Wireless Netw. (WiOpt)*, 2015, pp. 36–41.
- [28] M. Nilsson and H. Deknache, "Investigation of Bluetooth mesh and long range for IoT wearables," Bachelor thesis, Faculty Technol. Soc., Malmö Univ., Malmö, Sweden, 2018.
- [29] A. Cilfone et al., "Seamless IoT mobile sensing through Wi-Fi mesh networking," in *Wireless Mesh Networks for IoT and Smart Cities: Technologies and Applications*. London, U.K.: Inst. Eng. Technol., 2022, pp. 67–80.
- [30] "Buy a compute module 4." Accessed: Sep. 28, 2024. [Online]. Available: <https://www.raspberrypi.com/products/compute-module-4/?variant=raspberry-pi-cm4001000>
- [31] "RPF raspberry PI series." Accessed: Sep. 28, 2024. [Online]. Available: https://wikidevi.wi-cat.ru/RPF_Raspberry_Pi_series
- [32] "GW16146 802.11ah HaLow WiFi mini-PCIe card." Accessed: Sep. 28, 2024. [Online]. Available: <https://www.gateworks.com/products/mini-pcie-expansion-cards/gw16146-802-11ah-hallow-wifi-mini-pcie-card/>
- [33] "SX-NEWAH: Industry's first 802.11ah Wi-Fi solution for IoT devices." Accessed: Sep. 28, 2024. [Online]. Available: <https://www.silextechnology.com/connectivity-solutions/embedded-wireless/sx-newah>
- [34] "NRC7292: World's first Wi-Fi HaLow + MCU SoC." Accessed: Sep. 28, 2024. [Online]. Available: <https://newracom.com/products/nrc7292>
- [35] "GW16146 802.11ah HaLow mini-PCIe radio module—Throughput and latency limitation." Accessed: Sep. 28, 2024. [Online]. Available: <https://trac.gateworks.com/wiki/expansion/gw16146>
- [36] "SAW band pass filter (Center frequency 902.5 MHz and band pass width 25 MHz)." Accessed: Sep. 28, 2024. [Online]. Available: <https://www.crystek.com/specification/filter/CBPF5-0902.pdf>
- [37] "W1063M: External/in-building antenna: Stick/ blades, connector mount, 868–928MHz swivel type Dipole antenna." Accessed: Sep. 28, 2024. [Online]. Available: <https://productfinder.pulseelectronics.com/api/open/part-attachments/datasheet/w1063m>
- [38] "NRC7292 software package for host mode (Linux OS)." Accessed: Sep. 28, 2024. [Online]. Available: https://github.com/newracom/nrc7292_sw_pkg
- [39] "NRC9292 application note (11s mesh)." Accessed: Sep. 28, 2024. [Online]. Available: https://github.com/newracom/nrc7292_sw_pkg/blob/master/package/doc/AN-7292-007-11s_mesh_network.pdf
- [40] J. L. E. K. Fendji and S. D. Samo, "Energy and performance evaluation of reactive, proactive, and hybrid routing protocols in wireless mesh network," 2019, *arXiv:1903.06875*.
- [41] "B.A.T.M.A.N. advanced documentation overview." Accessed: Nov. 4, 2024. [Online]. Available: <https://www.open-mesh.org/projects/batman-adv/wiki>
- [42] B. Sliwa, S. Falten, and C. Wietfeld, "Performance evaluation and optimization of B.A.T.M.A.N. V routing for aerial and ground-based mobile ad-hoc networks," in *Proc. IEEE 89th Veh. Technol. Conf. (VTC-spring)*, 2019, pp. 1–7.
- [43] "GW16146 802.11ah HaLow mini-PCIe radio module." Accessed: Sep. 28, 2024. [Online]. Available: <https://trac.gateworks.com/wiki/expansion/gw16146>
- [44] K. K. Thangadurai, M. Prakash, M. Baddeley, A. Pandey, and K. M. Sivalingam, "Extending boundaries with WiLong: A field study on long-range Wi-Fi mesh custom solution," in *Proc. IEEE 49th Conf. Local Comput. Netw. (LCN)*, 2024, pp. 1–9.

- [45] “MCS index, modulation and coding index,” Accessed: Nov. 4, 2024. [Online]. Available: <https://mcsindex.net/>
- [46] “Industrial WiFi transceivers—NM-DB-2 & NM-DB-3.” Accessed: Sep. 28, 2024. [Online]. Available: <https://doodlelabs.com/datasheets/industrial-wifi-transceivers-nm-db-2-nm-db-3-datasheet/>
- [47] “3.4 indoor MIMO channel models.” Accessed: Dec. 25, 2024. [Online]. Available: <https://mentor.ieee.org/802.11/dcn/11/11-11-0968-04-00ah-channel-model-text.docx>
- [48] “Meet pixel 8 and pixel 8 pro, our newest phones,” Accessed: Sep. 28, 2024. [Online]. Available: <https://blog.google/products/pixel/google-pixel-8-pro/>
- [49] “Element | secure collaboration and messaging,” Accessed: Sep. 28, 2024. [Online]. Available: <https://element.io/>
- [50] “Dendrite matrix server.” Accessed: Sep. 28, 2024. [Online]. Available: <https://github.com/matrix-org/dendrite>
- [51] B. Jansen, T. Goodwin, V. Gupta, F. Kuipers, and G. Zussman, “Performance evaluation of WebRTC-based video conferencing,” *ACM SIGMETRICS Perform. Eval. Rev.*, vol. 45, no. 3, pp. 56–68, 2018.
- [52] A. Dawid and P. Buchwald, “Performance of modern video codecs in real-time communication WebRTC protocol,” in *Proc. Int. Conf. Dependability Complex Syst.*, 2022, pp. 32–41.
- [53] “iPerf—Download iPerf3 and original iPerf pre-compiled binaries,” Accessed: Sep. 28, 2024. [Online]. Available: <https://iperf.fr/iperf-download.php>
- [54] “ITU-T standards and recommendations.” [Online]. Available: <https://citeserx.ist.psu.edu/document?repid=rep1&type=pdf&doi=1c633c62f24869df4da7f04bd80bb2f30e8070df>
- [55] K. K. Thangadorai, K. M. Sivalingam, and K. Murugesan, “Poster: A multi-radio aware mesh platform for resilient human-to-human communication,” in *Proc. 21st Int. Conf. Embedded Wireless Syst. Netw.*, 2024, pp. 1–2.
- [56] “Using UDP multicast with GStreamer.” Accessed: Sep. 28, 2024. [Online]. Available: https://developer.ridgerun.com/wiki/index.php/Using_UDP_Multicast_with_GStreamer
- [57] “Multicast-optimizations—Batman-adv,” Accessed: Nov. 14, 2024. [Online]. Available: <https://www.open-mesh.org/projects/batman-adv/wiki/Multicast-optimizations>
- [58] Y.-G. Park et al., “Analysis of Wi-Fi HaLow device interference to LTE user equipment,” *J. Commun.*, vol. 15, no. 1, pp. 58–64, 2020.
- [59] “TDRA national frequency plan,” Accessed: Sep. 28, 2024. [Online]. Available: <https://tdra.gov.ae/en/test/national-frequency-plan>
- [60] “United Arab Emirates 5G—NR, 4G,” Accessed: Nov. 23, 2024. [Online]. Available: <https://www.spectrum-tracker.com/United-Arab-Emirates>
- [61] “SOL8SDR-M—Domo tactical communications.” Accessed: Sep. 28, 2024. [Online]. Available: <https://www.domotactical.com/assets/downloads/Datasheets/SOL8SDR-M-SOLO8-SDR-OEM-Module.pdf>



KAVIN KUMAR THANGADORAI (Member, IEEE) received the B.Tech. degree in information technology from Anna University, Chennai, India, in 2006, and the M.Tech. degree in computer science and engineering from the International Institute of Information Technology, Bengaluru, India, in 2018. He is currently pursuing the Ph.D. degree with the Indian Institute of Technology Madras. He has over 18 years of experience in research and development focused on Wi-Fi protocols, standards, and solutions across mobile, Wi-Fi routers, and embedded devices. He is a Lead Researcher with the Technology Innovation Institute, Abu Dhabi, UAE, specializing in long-range wireless communication, including Wi-Fi, HaLow, LoRa, and software-defined radio. Previously, he served as an Architect with Samsung R&D Institute India, Bengaluru, where he led the Wi-Fi team. He has authored eight articles and holds over 35 patents. He is professionally certified as a Certified Wireless Analysis Professional and a Certified Wireless Security Professional. His research interests include next-generation adaptive and intelligent Wi-Fi networks leveraging machine learning.



KRISHNA M. SIVALINGAM (Fellow, IEEE) received the B.E. degree from the Anna University’s College of Engineering Guindy, Chennai, India, in 1988, and the M.S. and Ph.D. degrees in computer science from SUNY Buffalo, Buffalo, NY, USA, in 1990 and 1994, respectively. He is the Institute Chair Professor with the CSE Department, Indian Institute of Technology Madras, Chennai. From 1994 to 2007, he was a Faculty Member of the University of Maryland at Baltimore County, Baltimore, MD, USA; Washington State University, Pullman, WA, USA; and University of North Carolina Greensboro, Greensboro, NC, USA. His research interests include computer networks and wireless networks. He has served as the Editor-in-Chief for *Photonic Network Communications* (Springer) and *EAI Endorsed Transactions on Future Internet* and is currently an Editorial Board Member of IEEE NETWORKING LETTERS. He is an INAE Fellow and an ACM Distinguished Scientist.



ANSHUL PANDEY (Member, IEEE) received the B.Tech. degree in ECE from the Indian Institute of Information Technology Design and Manufacturing, Jabalpur, India, in 2012, the M.Tech. degree in advanced networks from the Indian Institute of Information Technology and Management, Gwalior, India, in 2016, and the Ph.D. degree from the Department of Electronics and Communication Engineering, Indian Institute of Information Technology Allahabad, India, in 2021. He is a Senior Researcher with the Secure

Systems Research Center, Technology Innovation Institute, Abu Dhabi, UAE. He has authored over 35 publications in prestigious journals and conferences. His research interests include cooperative communications, wireless communications and security, physical-layer security, RIS, and signal processing. He is a reviewer of several reputed IEEE journals and transactions and has been a TPC member of IEEE conferences, including WCNC, VTC-Spring, and ICC.



KUMAR MURUGESAN received the B.Tech. degree in electronics and communication from Anna University, India, in 2004, and the M.Tech. degree in computer science and engineering from the International Institute of Information Technology, Bengaluru, India, in 2017. He has over 17 years of experience in research and development (R&D) focused on IEEE 802.11 Wi-Fi, network security, and 802.15.4 Thread Networking. He is a Lead Researcher with the Technology Innovation Institute, Abu Dhabi, UAE, specializing in wireless mesh networks, including OLSR and batman-adv routing protocols on Wi-Fi and HaLow-based devices. Previously, he worked as an Architect with Samsung R&D Institute India, Bengaluru, contributing to various wireless and network security projects. He holds ten patents in the connectivity domain and has authored six technical publications, significantly contributing to the field of network security. He is also a Certified Wireless Security Professional and a Certified Wireless Network Administrator.



MADHAN RAJ KANAGARATHINAM (Senior Member, IEEE) received the B.E. degree in computer science and engineering from Anna University, Chennai, India, in 2012, and the M.S. and Ph.D. degrees from the Indian Institute of Technology (IIT) Madras. He has ten years of experience designing and developing TCP/IP protocols, multi-path TCP, and UNIX-flavored operating systems. He is a Software Architect with Samsung R&D Institute India, Bengaluru. He is the author of 20 articles and more than 40 inventions. He also won IEEE Bangalore Young Technologist of the Year in 2020.